



REPORT SNO 5497-2007

# Particle affinity and bio-availability of PAHs associated with coal tar pitch



**Main Office**

Gaustadalléen 21  
 N-0349 Oslo, Norway  
 Phone (47) 22 18 51 00  
 Telefax (47) 22 18 52 00  
 Internet: www.niva.no

**Regional Office, Sørlandet**

Televeien 3  
 N-4879 Grimstad, Norway  
 Phone (47) 22 18 51 00  
 Telefax (47) 37 04 45 13

**Regional Office, Østlandet**

Sandvikaveien 41  
 N-2312 Ottestad, Norway  
 Phone (47) 22 18 51 00  
 Telefax (47) 62 57 66 53

**Regional Office, Vestlandet**

P.O.Box 2026  
 N-5817 Bergen, Norway  
 Phone (47) 22 18 51 00  
 Telefax (47) 55 30 22 51

**Akvaplan-NIVA A/S**

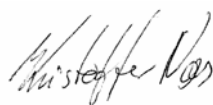
N-9005 Tromsø, Norway  
 Phone (47) 77 68 52 80  
 Telefax (47) 77 68 05 09

Title Particle affinity and bioavailability of PAHs associated with coal tar pitch	Serial No. 5497-2007	Date November 19, 2007
	Report No. Sub-No. 26066	Pages Price 64
Author(s) Anders Ruus Olav Bøyum Merete Grung Kristoffer Næs	Topic group Contaminants in the marine environment	Distribution Free
	Geographical area Norway/Sweden	Printed NIVA

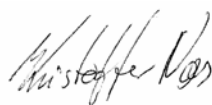
Client(s) Norsk Hydro, Elkem Aluminium Mosjøen, Kubickenberg Aluminium AB	Client ref. Bernt Malme/ Svein Harry Samulesen
--	---

**Abstract:** This project has investigated the particle affinity and bioavailability of coal tar pitch related PAHs from sediments outside several Nordic aluminium smelters using the Söderberg technology. Passive samplers (POM) have been used for assessing water-sediment partitioning for PAHs and actual bioaccumulation has been addressed in an experimental setup. The results showed that the PAHs associated with the sediments in the vicinity of the smelters were stronger (a median factor of at least a magnitude) adsorbed/absorbed to the particles than free energy relationship implies. This further implies that the bioavailable fraction is correspondingly lower, and one would expect lower bioaccumulated concentrations. The accumulated concentrations measured in *Nereis diversicolor* and *Hinia reticulata* were in fact very similar to biota concentrations expected based on the POM-deduced sediment-water partitioning coefficients. Thus, the measured biota to sediment accumulation factors (BSAFs) agreed also very well with those expected from the POM-deduced sediment-water partitioning coefficients. On the other hand, this good correspondence was not observed for the third species, the bivalve *Nuculoma tenuis*. There were however logistical intractabilities connected to this species biology and size that render it probable that particulate sedimentary matter contaminated the *Nuculoma* tissues analyses. The uncertainties associated with *Nuculoma tenuis* render the interpretations somewhat inconclusive for this species, and further investigations would be necessary to eliminate the uncertainties.

4 keywords, Norwegian	4 keywords, English
1. PAH	1. PAHs
2. Aluminiumsverk	2. Aluminium plants
3. Partikkeltilknytning	3. Particle association
4. Biotilgjengelighet	4. Bioavailability



Kristoffer Næs  
Project manager



Kristoffer Næs  
Research manager



Jarle Nygard  
Strategy Director

**Particle affinity and bioavailability of PAHs  
associated with coal tar pitch**

## Preface

This project has been performed by the Norwegian Institute for Water Research (NIVA) on contract with Norsk Hydro, Elkem Aluminium Mosjøen and Kubickenberg Aluminium AB.

Contact persons have been Bernt Malme, Steinar Frosta, Arne Magne Johannessen and Knut Erik Bjørseth at Norsk Hydro, Svein Harry Samuelsen and Helge Nes at Elkem Aluminium Mosjøen and Lena Wiig at Kubickenberg Aluminium AB.

At NIVA Kristoffer Næs has lead the project, Anders Ruus has been responsible for experimental setup and testing as well as most of the reporting, while Olav Bøyum has been in charge of the chemical analysis. In addition Eirin Sva, Harald Hasle Heiaas, Joachim Tørum Johansen, Merete Schøyen and Sigurd Øxnevad have assisted with fieldwork, as well as laboratorial, experimental and other and practical work. Some of the photos in this report were taken by Joachim Tørum Johansen.

We thank everyone for their contribution.

Oslo, November 19, 2007

*Kristoffer Næs*

---

# Contents

<b>Summary</b>	<b>6</b>
<b>Sammendrag</b>	<b>8</b>
<b>1. Introduction</b>	<b>10</b>
1.1 Background	10
1.2 Aims/Objectives	12
<b>2. Material and Methods</b>	<b>13</b>
2.1 Study areas/Sediments	13
2.2 Collection of control-sediment and organisms for bioaccumulation experiment	13
2.3 Homogenisation of sediments (field collected)	13
2.4 Preparation of sediment spiked with selected PAHs	13
2.5 POM-Solid Phase Extraction	14
2.5.1 Determination of sediment:water partitioning coefficients ( $K_d$ )	14
2.6 Bioaccumulation experiment	15
2.6.1 Organisms	15
2.6.2 Experimental setup	16
2.7 Chemical analyses	19
2.7.1 Analysis of total organic carbon (TOC) and black carbon (BC) in sediments	19
2.7.2 Analysis of PAHs in sediments	19
2.7.3 Analysis of PAHs in biota	19
2.7.4 Analysis of PAHs in POM	19
2.7.5 Analysis of other variables	20
2.7.6 Calculations	20
<b>3. Results</b>	<b>22</b>
3.1 Sediment to water partitioning coefficients ( $K_{ds}$ )	22
3.2 Biota concentrations (wet weight)	23
3.2.1 <i>Nereis diversicolor</i>	23
3.2.2 <i>Hinia reticulata</i>	25
3.2.3 <i>Nuculoma tenuis</i>	27
3.3 Biota to sediment accumulation factors (BSAFs)	29
3.3.1 <i>Nereis diversicolor</i>	29
3.3.2 <i>Hinia reticulata</i>	31
3.3.3 <i>Nuculoma tenuis</i>	33
3.4 PAH-profiles	35
<b>4. Discussion</b>	<b>40</b>
4.1 Conclusions	41

---

<b>5. References</b>	<b>42</b>
<b>6. Appendices</b>	<b>44</b>

## Summary

Polycyclic aromatic hydrocarbons (PAHs) have been and are a prioritized group of environmental contaminants in Norway and abroad. In Norway, the point sources have primarily been discharges from aluminium- and ferromanganese-smelters using the Söderberg anode in combination with sea-water scrubbing of pot room gas or flue gas from the baking furnaces at carbon plants. These discharges have been substantial and high concentrations of PAHs have been found in sediments and mussels in the vicinity of the smelters. Currently, focus on PAHs is especially with regard to planning remedial measures for the contaminated sediments, also in correspondence with implementation of the EU Water Framework Directive.

Although high concentrations of PAHs have been found in sediments in the vicinity of the smelters, the observed effects have been minor. It was hypothesized that the reason for this was that the PAH from smelters using the Söderberg anode was adsorbed to particles to a much higher degree than what was previously reported.

In Norway, a guidance manual is developed for assessing the environmental and human risk posed by contaminated sediments. In this manual, commonly accepted “template”-table values for the partitioning coefficients for PAHs are used in the risk algorithms. However, recently performed risk calculations for PAH-contaminated sediments near an aluminium production site as well as near an anode production facility for ferro-manganese industry in Southern Norway, showed that the empiric partitioning coefficients were substantially higher than the “template”-table values. A stronger PAH adsorption has a direct effect on the risk assessments, since it leads to less dissolution of PAHs from the sediments and thus less bioavailability.

The bioavailability of PAHs originating from coal tar pitch is also currently addressed in a draft risk assessment report from EU. In this document, the organic carbon-water partition coefficient is derived from octanol-water partitioning ( $K_{ow}$ ) using free-energy relationship.

To investigate further if the earlier observed PAH-adsorption also applies to sediments in the vicinity of other smelters, the Norwegian Institute for Water Research (NIVA) on contract with Norsk Hydro, Elkem Aluminium Mosjøen and Kubickenberg Aluminium AB has investigated the bioavailability of PAHs from sediments outside several Nordic smelters operating with Söderberg technology using passive samplers as well as investigating actual bioaccumulation in an experimental setup. The main aims were:

- Measurements of site specific partitioning coefficients for PAHs between sediment particles and water.
- Quantification of the accumulation of PAH in bottom dwelling organisms. The rationale for this is to show if high partitioning coefficients correspond with reduced bioavailability.

Solid phase extraction of polyoxymethylene (POM-SPE) used as passive samplers have been applied in partitioning coefficient determinations. A standard test system applying the polychaete *Nereis diversicolor* and gastropod *Hinia reticulata* was used in the bioaccumulation experiments. On request, a third species was also included, namely the bivalve *Nuculoma tenuis*.

The results from the POM-experiments showed that the PAHs associated with the sediments in the vicinity of the smelters were stronger (a median factor of at least a magnitude) adsorbed/absorbed to the particles than the free energy relationship implies. This further implies that the bioavailable fraction is correspondingly lower, and one would expect lower bioaccumulated concentrations. The accumulated concentrations measured in *Nereis diversicolor* and *Hinia reticulata* were in fact very

similar to biota concentrations expected based on the POM-deduced sediment-water partitioning coefficients ( $K_{d,s}$ ). Thus, the measured biota to sediment accumulation factors (BSAFs) agreed also very well with those expected from the POM-deduced  $K_{d,s}$ .

On the other hand, this good correspondence was not observed for the third species, *Nuculoma tenuis*. There were however logistical intractabilities connected to this species biology and size that render it probable that particulate sedimentary matter contaminated the *Nuculoma* tissues analyses. Exceptionally high PAH concentrations relative to the other two organisms and a PAH profile more similar to that of the sediments support this assumption. However, the many uncertainties associated with *Nuculoma tenuis* render the interpretations somewhat inconclusive for this species, and further investigations would be necessary to eliminate the uncertainties.



## Sammendrag

Polysykliske aromatiske hydrokarboner (PAH) har vært og er en prioritert gruppe av miljøgifter både i Norge og internasjonalt. I Norge har punktkildene i stor grad vært utslipp fra aluminium- og ferromanganverk med bruk av Søderberg-anoden, i kombinasjon med sjøvanns-“scrubbing” av avgasser fra smelteovenene på karbon-verkene. Utslippene fra disse verkene har vært betydelige og høye konsentrasjoner av PAH er funnet i sedimenter og skjell i nærområdene. I dag er PAH i fokus særlig i forbindelse med tiltaksplaner mot forurensede sedimenter og i forbindelse med implementeringen av EUs vannrammedirektiv.

Selv om det har blitt observert høye konsentrasjoner av PAH i sedimenter i nærområdene til verkene, har de observerte effektene vært små. Dette mente man kunne skyldes at PAH fra verk med Søderberganoden var sterkere partikkelbundet enn det som var rapportert i litteraturen.

I Norge er det utviklet en veileder for risikoberegning i forbindelse med tiltak mot forurensede sedimenter (nå under revidering). I denne anvendes allmenngyldige, sjablongmessige fordelingskoeffisienter for å beregne risikoen knyttet til PAH. NIVA har nylig gjennomført risikoberegninger knyttet til PAH-forurensede sedimenter nær et aluminiumsverk, samt i nærheten av en anodefabrikk for ferromanganindustrien i sør-Norge. Disse undersøkelsene viste at de empiriske fordelingskoeffisientene var vesentlig høyere enn de sjablongmessige tabell-verdiene. En sterkere PAH-adsorpsjon har direkte betydning for risikovurderinger, siden det fører til mindre PAH løst i vann og dermed lavere biotilgjengelighet.

Biotilgjengelighet av PAH fra kulltjærebeak er også berørt i et (utkast til et) risikovurderingsdokument fra EU. I dette dokumentet er karbon-vann-fordelingskoeffisienter utledet fra oktanol-vann-fordelingskoeffisienter ( $K_{OW}$ ) ved bruk av fri-energi-sammenheng.

For å videre undersøke om den tidligere observert PAH-adsorpsjonen også gjelder for sedimenter utenfor andre smelteverk, har NIVA på kontrakt fra Norsk Hydro, Elkem Aluminium Mosjøen og Kubickenberg Aluminium AB, undersøkt biotilgjengeligheten av PAH fra sedimenter utenfor flere nordiske smelteverk som opererer med Søderberg-teknologi. I disse undersøkelsene er passive prøvetakere benyttet og faktisk bioakkumulering er undersøkt ved hjelp av et spesialdesignet forsøksoppsett. Hovedmålene med undersøkelsen var:

- Målinger av stedsspesifikke fordelingskoeffisienter for PAH mellom sedimentpartikler og vannfasen
- Kvantifisering av akkumuleringen av PAH i bunnlevende organismer. Hensikten med dette var å se om høye fordelingskoeffisienter korresponderer med redusert biotilgjengelighet

Fastfaseekstraksjon av polyoksymetylen, benyttet som passiv prøvetaker, har vært anvendt i bestemmelser av likevekstfordelingskoeffisienter. Et standard testsystem med flerbørstemarken *Nereis diversicolor* og sneglen *Hinia reticulata* har vært brukt i bioakkumuleringsforsøkene. På etterspørsel ble også en tredje art inkludert, nemlig muslingen *Nuculoma tenuis*.

Resultatene fra POM-forsøkene viste at PAH tilknyttet sedimenter i nærheten av smelteverkene var sterkere (en median faktor på minst en størrelsesorden) adsorbent/absorbent til partiklene enn det som fri-energi-sammenheng skulle tilsi. Dette impliserer at den biotilgjengelige fraksjonen er tilsvarende lavere, og man skal kunne forvente lavere bioakkumulerte konsentrasjoner i organismer. De akkumulerte konsentrasjonene målt i *Nereis diversicolor* og *Hinia reticulata* var faktisk også veldig like de konsentrasjoner man skulle forvente i biota, basert på sediment-vann-fordelingskoeffisienter ( $K_d$ ), bestemt v.h.a. POM-SPE.

På den annen side, så kunne denne gode sammenhengen mellom forventet og faktisk målt akkumulert konsentrasjon ikke observeres for den tredje arten, muslingen *Nuculoma tenuis*. Det var imidlertid visse logistiske uregjerligheter forbundet med denne artens biologi og størrelse, som gjorde det mulig at partikulært materiale (med opphav i sedimentene) kunne ha forurenset vevsprøvene fra denne organismen. Eksepsjonelt høye PAH-konsentrasjoner, relativt til i de andre to artene, og en PAH-profil som lignet mer på helsediment støtter denne antagelsen. De mange usikkerhetene assosiert med *Nuculoma tenuis* gjør imidlertid tolkningene noe ufyllestgjørende for denne arten og ytterligere undersøkelser er nødvendig, dersom man vil disse usikkerhetene til livs.

# 1. Introduction

## 1.1 Background

Polycyclic aromatic hydrocarbons (PAHs) have been and are a prioritized group of environmental contaminants in Norway and abroad. In Norway, the point sources have primarily been discharges from aluminium- and ferromanganese-smelters using the Sjøderberg-anode in combination with sea-water scrubbing of pot room gas or flue gas from the baking furnaces at carbon plants. These discharges have been substantial and high concentrations of PAHs have been found in sediments and mussels in the vicinity of the smelters. Currently, focus on PAHs is especially with regard to planning remedial measures for the contaminated sediments, also in correspondence with implementation of the EU Water Framework Directive.

Although high concentrations of PAHs have been found in sediments in the vicinity of the smelters, the observed effects have been minor (Næs, 1998). It was hypothesized that the reason for this was that the PAH from smelters using the Sjøderberg-anode was adsorbed to particles to a much higher degree than what was reported. It is widely accepted that it is the freely dissolved fraction of pollutants that is available for interaction with biological tissues and thereby can cause bioaccumulation and/or biological effects. To test this, Næs et al. (1998) quantified PAHs in effluent- and recipient-water outside a Sjøderberg aluminium smelter in Southern Norway. The measurements showed that that the partitioning coefficients (i.e. the ratios of particle adsorbed PAHs to dissolved PAHs) were factors of 100-1000 higher than reported values (**Figure 1**).

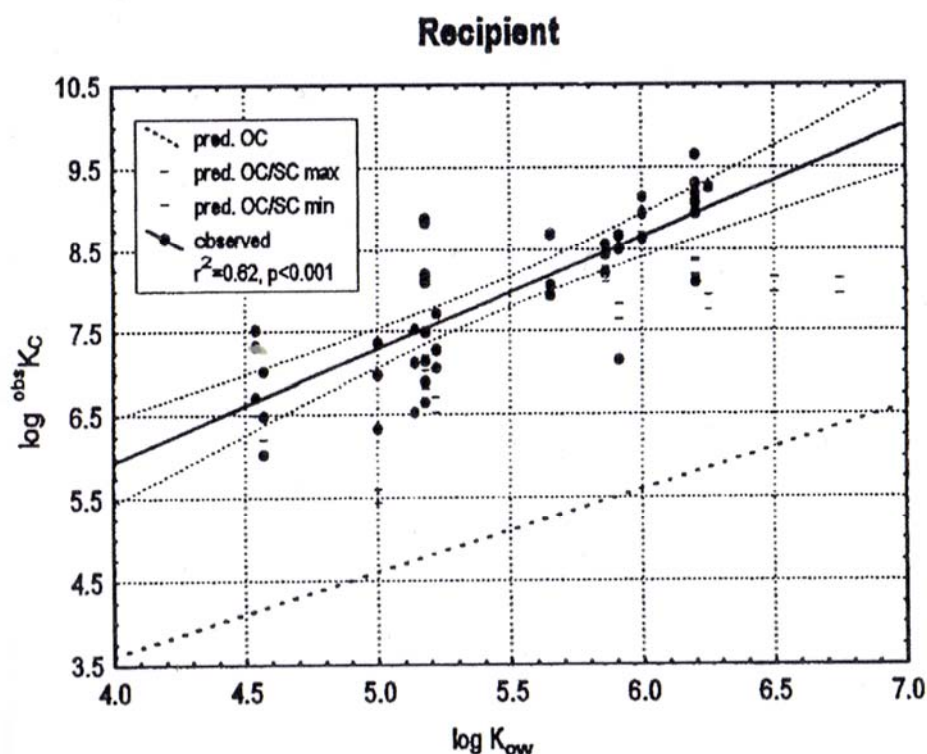


**Figure 1.** Logarithm of the observed partition coefficient of individual PAHs plotted against  $\log K_{ow}$  in the recipient sea water outside a Norwegian aluminium plant using the Söderberg technology. The linear regression lines with 95% confidence bands have also been plotted. The predicted relationship between  $\log K_{ow}$  and  $\log K_c$  based solely on organic carbon partitioning (predicted OC) and based on both soot carbon and organic carbon (predicted SC and OC) are shown (from Næs et al. 1998).

With regard to remedial measures for contaminated sediments, a guidance manual is developed for assessing the environmental and human risk in Norway (Breedveld et al., 2005). In this manual, commonly accepted “template”-table values for the partitioning coefficients for PAHs are used in the risk algorithms. Norwegian Institute for Water Research (NIVA) has recently performed risk calculations for PAH contaminated sediments near an aluminium production site as well as near an anode production facility for ferro-manganese industry in Southern Norway. In these projects site specific partitioning coefficients (and not use the “template”-table values) were measured. As expected, the empiric partitioning coefficients were substantially higher than the “template”-table values.

The results indicated that the PAHs were much stronger adsorbed to particles than assumed in the risk assessment tool. A stronger PAH adsorption has a direct effect on the risk assessments, since it leads to less dissolution of PAHs from the sediments and thus less bioavailability. The PAH-adsorption-results referred to above are confirmed by recent articles on the same topic (Cornelissen et al. 2005, Cornelissen et al. 2006, Khalil et al. 2006).

The bioavailability of PAHs originating from coal tar pitch is currently addressed in a draft risk assessment report (RAR) from EU. In this document, the organic carbon-water partition coefficient is derived from  $K_{ow}$ , using Free-energy relationship (following Karickhoff et al., 1979):

$$\log K_{oc} = \log K_{ow} - 0.21$$

The document references are made to other studies that have shown substantially higher adsorption to sediments (much due to the presence of soot-like materials; black carbon), that what can be deduced from the above equation. However, it is chosen to disregard these results in the draft RAR, since the implications for risk assessment could be difficult to interpret for several reasons. Furthermore, an interesting and comprehensive study by Rust et al. (2004a) showed that despite the effect of black carbon on the sorption of PAHs to sediments, the bioavailability did not seem to decrease significantly with increasing black carbon content. It should be noted, however, that the authors studied soot obtained from tail-pipes of diesel-powered vehicles, and the soot was then spiked with PAHs. The relevance to coal tar pitch is thus questionable, and the authors themselves stated that “further work is required to determine the extent to which these results can be generalized to other sources of soot carbon”.

## 1.2 Aims/Objectives

The risk assessments with regard to PAH-issues should be as accurate as possible, and it is therefore a need to further substantiate if the earlier observed PAH-adsorption also applies to sediments in the vicinity of other smelters. Such documentation would be of value in several contexts. It could *inter alia* form a basis for revision of the risk calculations for PAH with regard to remedial measures for contaminated sediments, it would strengthen the theory of limited bioavailability of PAH originating from coal tar pitch, it would be an important input with regard to marginal values for PAH in water proposed in the EU Water Framework Directive, it would give important input of how to monitor PAHs in water recourses, etc.

To further pursue this, NIVA took on a task to investigate the bioavailability of PAHs from sediments outside several Nordic smelters, using passive samplers for PAHs as well as investigating actual bioaccumulation in an experimental setup. The aims of the project were as follows:

1. Verify the partitioning constants for the passive samplers used in the measurements. This was laboratory work where the aim is to make certain that the NIVA performance corresponds with reported values in the literature.
2. Measurements of site specific partitioning coefficients for PAHs between sediment particles and water. These measurements were performed on sediments collected outside each of the smelters.
3. Quantification of the accumulation of PAH in bottom dwelling organisms. The rationale for this is to show if high partitioning coefficients correspond with reduced bioavailability (investigate correspondence to pt. 2, above).

The investigations are focused towards the sediment-water system. However, the results will also be applicable to the issues with regard to PAHs and particle affinity and bioavailability in other water-particle systems.

The ideas behind the present project were presented at the EU TC-NES meeting March 6<sup>th</sup>, 2006. Some views and advices were received. These were taken under consideration and attempts have been made to meet the requests put forward. An additional species was e.g. included in the experimental setup, and a clean sediment spiked with PAHs was introduced (as described in the following).

The International Council for Exploration of the Sea (ICES) is currently performing a passive sampling trail survey. Two of the smelter sites are the Norwegian entries to this testing. Here silicon rubber is used as passive sampler both for determination of the freely dissolved PAH concentration in pore water as well as in the water masses.

## 2. Material and Methods

### 2.1 Study areas/Sediments

Sediments were collected from four locations in Norway and one in Sweden. The sites represent the primary sea water recipients for aluminium smelters using the Söderberg technology. In this report, the sites are presented as Smelter A, B, C, D and E. At all locations sediments were sampled from one representative site, apart from one fjord where three sites in a gradient from the smelter were sampled (Smelter A, the three locations are named Smelter A1, A2 and A3). In addition, unpolluted sediments representing the control/reference were collected from a clean site in the outer Oslofjord. Finally, a spiked sediment (spiked with selected PAHs) was prepared based on samples from the control site. (see below).

The sediments were collected using a van Veed grab (0.1 m<sup>2</sup>). 10 litres of sediments were collected per site representing the upper 15 cm of the sediment. The sediments were relatively fine grained with the fraction less than 63 µm ranging from 30-96 per cent and total organic carbon from 0.4-6.8 per cent.

### 2.2 Collection of control-sediment and organisms for bioaccumulation experiment

The test-organisms (see below) *Nereis diversicolor* and *Hinia reticulata* were collected at the same location as the control sediments, Rambergbukta at Jeløya in the outer Oslofjord. *Nereis* were handpicked from sediment dug up using a shovel. *Hinia* were attracted using a crushed blue mussel (*Mytilus edulis*) as bait, and handpicked. *Nuculoma tenuis* were collected near Drøbak by the use of a 0.1 m<sup>2</sup> vanVeen-grab.

After an acclimation period in control sediments and the same water used in the experiments of approximately one week, twenty individuals of *N. diversicolor*, 10 individuals of *H. reticulata* and 8-9 individuals of *N. tenuis* were added to each test aquarium (see below).

### 2.3 Homogenisation of sediments (field collected)

The sediments were stored chilled (~4 °C) after collection. Before preparation they were homogenised 60–90 sec. by the use of a mechanical stirrer (paint mixer used for sediments only). Aliquotes were taken for chemical analyses, determination of particle:water-partitioning coefficients (K<sub>ds</sub>; by the use of POM-SPE), and the bioaccumulation experiment (see below).

### 2.4 Preparation of sediment spiked with selected PAHs

It was aimed to prepare a sediment spiked with selected PAHs to concentrations between 0.5 and 1 mg/kg (dry wt.) for each individual compound. Approximately 1 kg of wet clean reference/control sediment was dried at 100 °C for 48 h and sieved (1 mm). Approximately 0.005 g of each of the compounds **anthracene**, **phenanthrene**, **benzo(b)fluoranthene**, **pyrene**, **benzo(a)pyrene**, **dibenz(a,h)anthracene**, **fluoranthene**, **benzo(k)fluoranthene** and **indeno(1,2,3-cd)pyrene** were diluted in 100 ml dichloromethane. The solution was added to the dried sediment and shaken (approximately 15 h) before the solvent was evaporated. The spiked sediment was mixed into approximately 14 kg of wet (clean/same as “control”) sediment, first using a mechanical stirrer (treated as the field collected sediments; above), and then in a “cement mixer” for 48 h.

## 2.5 POM-Solid Phase Extraction

### 2.5.1 Determination of sediment:water partitioning coefficients ( $K_d$ )

To elucidate the particle association and bioavailability, analyses of freely dissolved fractions of PAHs in the sediments were performed with a Solid Phase Extraction (SPE) method using Plastic polyoxymethylene (POM) (Jonker & Koelmans, 2001; Cornelissen & Gustafsson, 2004; see reference for details). From the results, partitioning coefficients between the particular phase and the water phase ( $K_d$ ) were calculated. Dichloromethane was used to extract the PAHs from the POM-strips (1 week) before analysis. Prior to the application of the method to the sediments, the partitioning coefficient between the POM material and water ( $K_{pom}$ ) was tested experimentally (with water spiked with PAH-standards). Very good correspondence with the coefficients published by Jonker & Koelmans (2001) were obtained (especially for the compounds phenanthrene, anthracene, fluoranthene, pyrene, benzo(*a*)anthracene, chrysene, benzo(*a*)pyrene and indeno(*1,2,3-cd*)pyrene).

The  $K_d$ -coefficients for sediments were determined as follows: For each of the sediments ~2 g sediment (wet) and ~1 g POM (both weighed accurately) were transferred to bottles and added 300 ml distilled water (containing a biocide; as described in Jonker and Koelmans 2001). In addition a bottle was only added POM and water (blank). Subsequently all bottles were placed on a shaker. After 30 days the POM was removed (using forceps) and carefully rinsed in distilled water. It was then transferred to a test tube, before 40 ml dichloromethane and internal standards (200 ng of each of the deuterated PAH components used at the laboratory) were added. The test tubes were sealed and placed on a shaker for 7 days. The extract was decanted to another test tube, before the extract was evaporated to 200  $\mu$ l prior to chemical analyses GC-MS (See below). The detection limit was 2 ng/POM.

The PAH mass balance in the three-phase-system: particles  $\Leftrightarrow$  water  $\Leftrightarrow$  POM can be expressed as follows (Jonker & Koelmans 2001):

$$Q_{\text{tot}} = C_s M_s + C_w V_w + C_p M_p$$

where:

$Q_{\text{tot}}$  is the total amount of PAH in the system ( $\mu$ g; corresponds to the amount analysed in the added sediment).

$C_s$  is the concentration of the compound in the sediment ( $\mu$ g/kg dry wt).

$M_s$  is the mass of the added sediment (kg dry wt)

$C_w$  is the concentration in the water ( $\mu$ g/L; unknown)

$V_w$  is the volume of the added water (L)

$C_p$  is the concentration in the POM ( $\mu$ g/kg; analysed)

$M_p$  is the mass of POM (kg)

The following partition coefficients exist for the system:

$$K_d = C_s / C_w$$

$$K_p = C_p / C_w$$

Therefore, one can express:

$$K_d = \frac{1}{M_s} \left( \frac{K_p Q_{\text{tot}}}{C_p} - M_p K_p - V_w \right)$$

Values for  $K_p$  for several PAHs are given by Jonker & Koelmans (2001). These authors also show that  $K_p$  is proportional to the octanol:water-partitioning coefficient ( $K_{ow}$ ) of the compounds:  
 $\log K_p = 0,72 \times \log K_{ow} + 0,39$ .

## 2.6 Bioaccumulation experiment

In the following, a system for direct measurements of bioaccumulation is described. Analogous bioavailability studies have been conducted in several countries, in most cases as a tool in the assessment of the environmental risk of dredged sediment. The most comprehensive documentation from such tests has been produced by the U.S. Environmental Protection Agency (Lee et al., 1991).

### 2.6.1 Organisms

Organisms used in the experiments were the ragworm *Nereis diversicolor* (**Figure 2**; Polychaeta), the netted dog whelk *Hinia reticulata* (**Figure 3**; Gastropoda) and the protobranch bivalve *Nuculoma tenuis* (**Figure 4**). We have earlier used *N. diversicolor* and *H. reticulata* in similar bioaccumulation tests on a number of occasions (e.g. Ruus et al. 2005). On request a third species was included, namely *N. tenuis*. The rationale for using these species is that they are intimately interacted with the sediment, possible to obtain in sufficient numbers, and possible to hold in aquaria for extended periods.



**Figure 2.** Picture of the polychaete *Nereis diversicolor*. These individuals are ready to be added to the test aquaria.

*Nereis diversicolor* is common along the coasts of Europe, from the Mediterranean to Helgeland (Mid Norway), and in the Baltic Sea. It is found primarily in shallow waters, where it can occur in dense populations. *Hinia reticulata* is also found in shallow waters and is common from the Canary Islands and the Azores in the south, to Lofoten in the north. Both species prefer sandy or muddy sediment and are tolerant to low salinities. *N. diversicolor* is omnivorous, ingesting also sediment, while *H. reticulata* is primarily a scavenger and a predator. *N. diversicolor* is one of the most studied marine invertebrates and has also been used in other bioaccumulation studies (Fowler et al., 1978; Goerke, 1984).



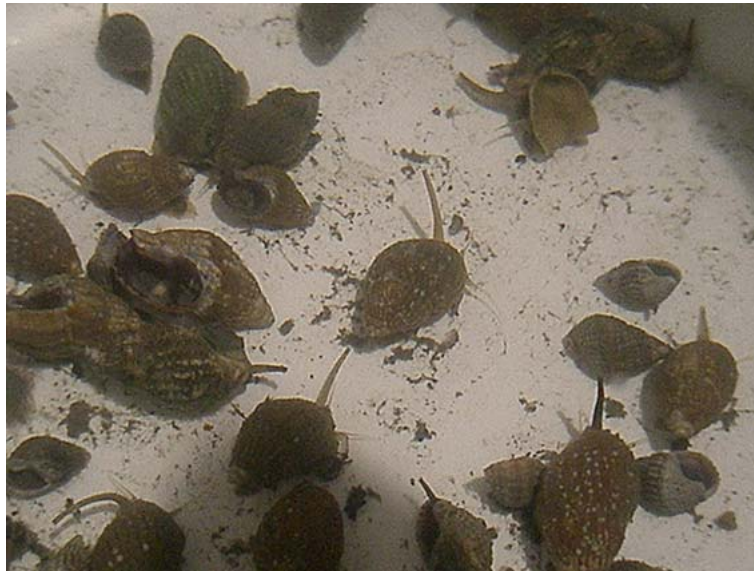


**Figure 3.** Picture of the netted dogwhelk, *Hinia reticulata*. These individuals are ready to be added to the test aquaria.

*Nuculoma tenuis* is a primitive protobranch bivalve, fairly common in the Skagerrak and northern Kattegat. It is very common in the southern Kattegat, deeper than 10 m. *N. tenuis* is a selective sub-surface deposit feeder. It feeds by the use of ciliated tentacles which are extended into the substrate. Particles are carried to the labial palps for sorting, prior to ingestion. Thus, the gills are primarily respiratory organs (Gosling, 2003).



**Figure 4.** Picture of the protobranch bivalve, *Nuculoma tenuis*. These individuals are ready to be added to the test aquaria.

### 2.6.2 Experimental setup

The experimental setup was established a decade ago and described on several occasions (e.g. Hylland 1996; Ruus et al. 2005). In short, the setup is as follows: The exposure experiments were performed in

---

all-welded glass aquaria (15 × 20 × 22 cm; holding 5 litres of water/sediment), placed on a water-bath table with header tanks (secondary; with the same number of outlets as the number of aquaria; **Figure 5**). Each aquarium had an outlet 5 cm below the top, covered with a plastic netting (200 µm) to prevent organisms from escaping. To maintain a proper flow through, two plexi glass partition walls were attached in each aquarium. By the use of a main header tank, a constant, uniform water supply was maintained in all aquaria. The water supplied to the aquaria was pumped from 60m depth outside NIVA's marine research station at Solbergstrand, Oslofjord. The same water was supplied to the water bath to uphold a stable temperature in the aquaria. Temperature and salinity were logged with WTW electrodes every minute in the primary header tank and measured to 8.2-9.4 °C and 33.9-34.3 ‰, respectively.

Three replicate aquaria were used for each test sediment. The duration of the accumulation period was 28 days as recommended by Lee et al. (1991), since it should result in steady-state tissue residues.



**Figure 5.** Picture of parts of the experimental setup, after initiation of the bioaccumulation experiment.

By termination of the experiment, the test organisms were retrieved from the aquaria (**Figure 6**). The polychaetes were transferred to beakers of sea water in which they were held for 6 to 8 hours to empty all remnants of sediments from the intestines before freezing (−20 °C) in glass containers. The soft parts of the gastropods were separated from their hard shell using a nut-cracker. The soft parts were then rinsed in seawater and transferred to glass containers then stored at −20 °C until chemical analysis. Individuals of *Nuculoma* were rinsed in seawater and frozen (−20 °C) in glass containers. All individuals of the same species from each aquarium were pooled into one sample.



**Figure 6.** Picture of one experimental unit (aquarium) before termination of the bioaccumulation experiment. The shell of a netted dogwhelk (*Hinia reticulata*) is visible on the sediment surface. Burrows of the polychaete *Nereis diversicolor* in the sediment are also visible.

Upon thawing (prior to analysis), the soft parts of *N. tenuis* were excised from the shells. In this process, it was discovered that approximately 40% of the individuals were empty/dead. These were also the largest/oldest individuals. This was the case for all aquaria including the control sediment. The dead mussels were obviously empty shells from the field, but we also found some indications of *H. reticulata* preying on *N. tenuis* (a few shells only; **Figure 7**). To optimize the amount of biomass for analysis, the triplicates were pooled for this organism prior to analysis.



**Figure 7.** Empty shells of *Nuculoma tenuis* after termination of the bioaccumulation experiment. A few shells showed signs of possible predation by *Hinia reticulata* (holes in shell).

## 2.7 Chemical analyses

All sediments (including the reference/control and the spiked sediment) were analysed for PAH compounds, particle size fraction (<63 µm), total organic content and black carbon content at NIVA's laboratory, accredited by the Norwegian Accreditation as a testing laboratory according to the requirements of NS-EN ISO/IEC 17025 (2000). Analytical standards of the laboratory are also certified by the participation in international calibration tests, including QUASIMEME twice per year.

### 2.7.1 Analysis of total organic carbon (TOC) and black carbon (BC) in sediments

The sediments were freeze-dried, crushed and acidified (1N HCl). Subsequently the sediments were analysed for total organic carbon (TOC) by catalytic combustion at 1800 °C in an elemental analyser. The black carbon (BC) content was analysed by a method described by Cornelissen and Gustavsson (2004), first by heating the sediment (375 °C) for 18 hours in excess of air, and then following the same procedure as for TOC.

### 2.7.2 Analysis of PAHs in sediments

The sediment samples were homogenised and added internal standards. The PAHs were then extracted with dichloromethane and cyclohexane (1:1, vol/vol) by Accelerated Solvent Extraction (ASE) (Dionex ASE-200; Dionex Corp., Sunnyvale, CA, USA) at a temperature of 100 °C and a pressure of 2000 psi. The further cleaning of the extracts and GC/MS analysis was as described for biota, below. The certified reference material used when analysing sediment was SRM 1944.

### 2.7.3 Analysis of PAHs in biota

Samples of polychaetes and gastropods were homogenized, using an ultra Turrax™. The soft parts of the individual bivalves (*Nuculoma*) were small and needed no homogenization before extraction. Subsequently, the samples were added internal standards (200 ng each of naphthalene d8, acenaphthene d8, phenanthrene d10, chrysene d12, perylene d12, and anthracene d10) and saponified. The PAHs were extracted with n-pentane and dried over sodium sulphate. The extraction volume was reduced, solvent exchanged to dichloromethane, and the extracts were cleaned by gel permeation chromatography (GPC) and solvent exchanged to cyclohexane. The extracts were analysed by gas chromatography and mass spectrometry (GC/MS). The MS detector was operated in selected ion monitoring mode (SIM), and the analyte concentrations in the standard solutions were in the range 2 to 5000 ng/µl. The GC was equipped with a 30 m J&W DB-5MS (stationary phase of 5% phenyl polyoxilane) column (0.25 mm i.d. and 0.25 µm film thickness), and an inlet operated in the splitless mode. The initial column temperature was 60 °C, which after two minutes was raised to 250 °C at a rate of 7 °C/min and thereafter raised to 310 °C at a rate of 15 °C/min. The injector temperature was 300 °C, the transfer line temperature 280 °C and the MS source temperature 230 °C. The column flow rate was 1.2 ml/min. Quantification of individual components was performed by using the internal standard method. Standard laboratory procedure is to subtract any PAH component concentrations detected in blanks (solvent and internal standards) from all sample concentrations. The quality of each sample series was controlled by analysing certified reference material (SRM 2977).

### 2.7.4 Analysis of PAHs in POM

The extracts from the POM material (see above) were analysed for PAHs by GC/MS as described for the biota extracts (above).

### 2.7.5 Analysis of other variables

Total dry matter in the sediments was analysed gravimetrically.

Aliquots of the homogenized material (*Nereis* and *Hinia*) or an individual mussel (*Nucoloma*) from each of the groups were used to determine the lipid content gravimetrically, after lipid extraction (cyclohexane and acetone).

Proportion (weight percentage) of particles with size <63 µm was analysed according to the methods described by Krumbein and Pettijohn (1938).

### 2.7.6 Calculations

a.) The organic carbon-water partition coefficients were derived from  $K_{ow}$ s, using Free-energy relationship (following Karickhoff et al., 1979), as described in the RAR (and the EU Technical Guidance Document; TGD):

$$\log K_{oc} = \log K_{ow} - 0.21$$

The  $K_{ow}$ s (octanol:water-partitioning coefficients) used were the same as those used in the RAR.

These were compared with the  $K_{oc}$ s deduced using the POM method.

b.) Expected biota concentrations (wet weight) were then calculated using the sediment concentrations,  $K_d$  (sediment water partitioning coefficient;  $K_d = K_{oc} \times f_{oc}$ ;  $f_{oc}$  is the fraction of organic content in the sediment) and BCF (bioconcentration factors).

$$C_{biota} = (C_s/K_d) \times BCF$$

The bioconcentration factors were deduced using the equations described in the TGD:

For  $\log K_{ow}$  2-6:

$$\log BCF = 0.85 \times \log K_{ow} - 0.70$$

For  $\log K_{ow} > 6$ :

$$\log BCF = -0.20 \times \log K_{ow}^2 + 2.74 \times \log K_{ow} - 4.72$$

Expected biota concentrations calculated using the free-energy relationship (Karickhoff) deduced  $K_d$ s and expected biota concentrations calculated using the POM-deduced  $K_d$ s were both compared with the actual biota concentrations measured in the species from the experimental setup.

c.) A less crude approach was also pursued. To account for the amount of organic carbon in the sediment and amount of lipid in the organisms, biota to sediment factors (BSAF)s were calculated.

$BSAF = \frac{C_{lipid}}{C_{OC}}$ , where  $C_{lipid}$  is the lipid normalized concentration in the organism, and  $C_{OC}$  is the organic carbon normalized concentration in the sediment.

Expected BSAFs were calculated from the free-energy relationship (Karickhoff) deduced  $K_{oc}$ s, assuming the partitioning coefficient between organism lipids and water equals  $K_{ow}$  ( $K_{lipid} = K_{ow}$ ):

$\log K_{oc} = \log K_{ow} - 0.21$  or  $K_{oc} = 0.62 K_{ow}$  (Karickhoff et al., 1979)

and since:

$$K_{lipid} = \frac{C_{lipid}}{C_W}, K_{OC} = \frac{C_{OC}}{C_W} \text{ and } C_{OC} = \frac{C_S}{f_{OC}},$$

BSAF equals:

$$BSAF = \frac{K_{ow} \cdot C_W}{0.62 \cdot K_{ow} \cdot C_W} = 1.62$$

Expected BSAFs were also calculated from the POM-deduced  $K_d$ s

$$BSAF = \frac{C_{lipid}}{C_{OC}} = \frac{K_{lipid} \cdot C_W}{\left( \frac{C_S}{f_{OC}} \right)} \text{ where } C_W = C_S / K_d$$

Where  $C_W$  is the concentration in water and  $C_S$  is the concentration in sediment.

The two above mentioned calculated expected BSAFs were then compared to the BSAFs calculated from actual measured concentrations in organisms and sediments.

### 3. Results

#### 3.1 Sediment to water partitioning coefficients ( $K_{ds}$ )

Sediment:water-partitioning coefficients ( $K_{ds}$ ) deduced using the POM-SPE method were higher than those derived from  $K_{ow}$ , using Free-energy relationship (following Karickhoff et al., 1979). Comparing the organic carbon normalized  $K_{ds}$  (in other words  $K_{ocs}$ ), the  $K_{ocs}$  deduced using the POM method were a factor **4 – 747** (median = **26**) higher, looking at all sediment and all PAH compounds (**Figure 8**).  $K_{ocs}$  could not be deduced using the POM-method for the few compounds with molecular weight less than phenanthrene. The individual values are also presented in Appendix F.

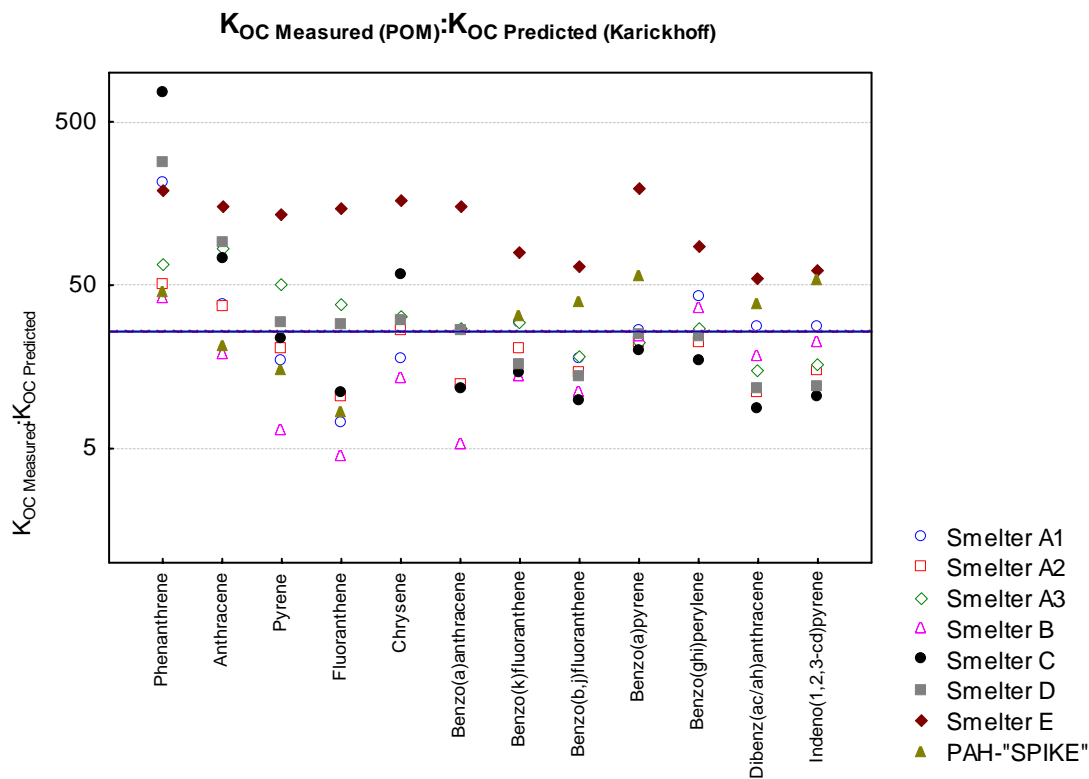


**Figure 8.** The ratio between the organic carbon:water-partitioning coefficient ( $K_{oc}$ ) deduced by POM-solid phase extraction and the predicted  $K_{oc}$  derived from  $K_{ow}$ , using free-energy relationship (following Karickhoff et al., 1979). The ratio is presented for all sediments and all PAHs (from phenanthrene) presented from left to right with increasing  $K_{ow}$ s. The median (26) is presented by a blue line. Note logarithmic scale.

These results imply lower pore-water concentrations to be compared with predicted no adverse effect levels (PNECs) in risk assessment. Furthermore, it would imply lower expected bioavailable fractions for bioaccumulation. **Figure 8** shows that the variability is great between the sediments for phenanthrene. Furthermore, it shows that the PAHs in the sediment especially from Smelter E are apparently much stronger adsorbed to the particles that the Karickhoff free-energy relationship would imply.

The  $K_{OC}$ s measured by the use of POM-SPE showed a significant linear relationship with the  $K_{OW}$ s (**Figure 9**;  $P < 0.000001$ ;  $R^2 = 0.66$ ). This figure also shows a higher  $\log K_{OC} : \log K_{OW}$ -ratio than the Karickhoff et al. (1979) relationship. The largest discrepancy, compared with the Karickhoff et al. (1979)-deduced  $K_{OC}$ s appear for the PAHs with the lowest  $K_{OW}$ s (**Figure 9**).

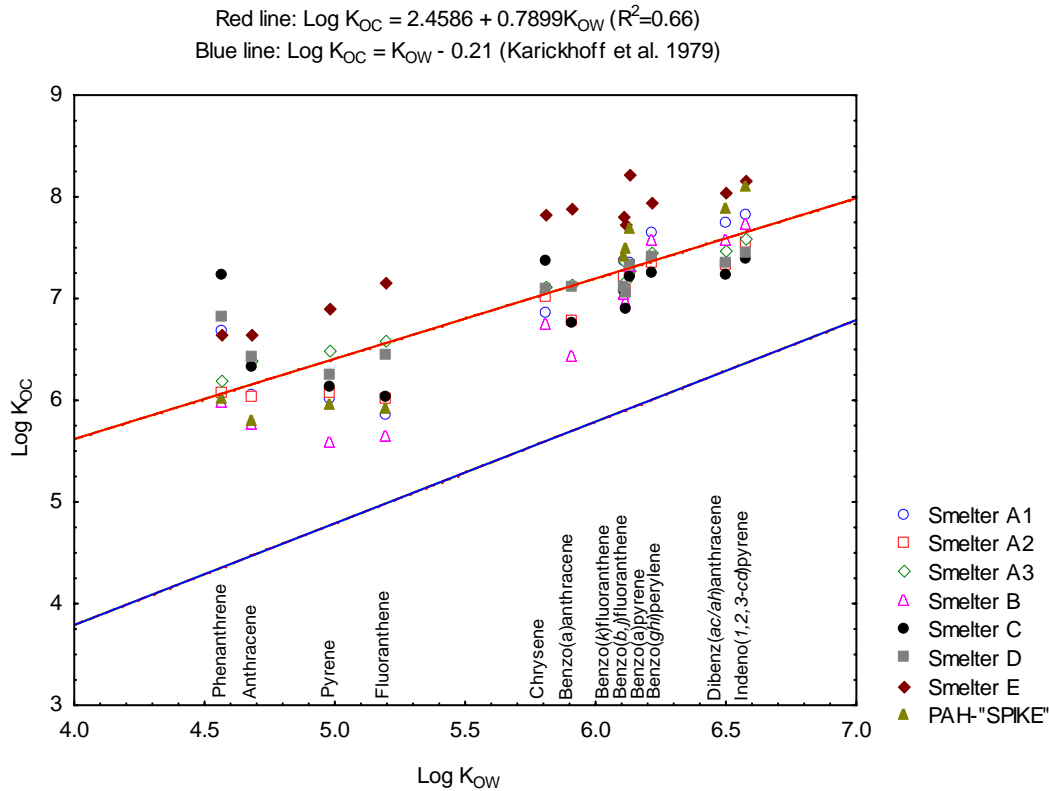


**Figure 9.** The logarithms ( $\text{Log}_{10}$ ) of octanol:water-partitioning coefficients ( $K_{OW}$ ) plotted against the logarithms of organic carbon:water-partitioning coefficients ( $K_{OC}$ ) determined by the use of POM solid phase extraction. All sediments and all PAHs (from phenanthrene) are included. The red line represents the linear regression from all data points. The blue line represents the Karickhoff et al. (1979) free energy relationship.

### 3.2 Biota concentrations (wet weight)

All individual biota concentrations (predicted using the various methods described above and actual measured concentrations in all species) are presented in Appendices B-D and H-I.

#### 3.2.1 *Nereis diversicolor*

Expected biota concentrations calculated from  $K_{dS}$  deduced using POM-SPE, sediment concentrations and bioconcentration factors (BCFs; see pt. b. in paragraph 2.7.6 *Calculations*, above) corresponded good with the concentrations actually measured in *N. diversicolor*. More specific, the expected concentrations were a factor **0.3 (0.5 if the PAH-“SPIKE” sediment is excluded) to 24** (median = **4.0**) higher than the actual accumulated concentrations (varying with PAH compound and sediment; **Figure 10**). No specific sediment or PAH stands out showing any particular discrepancy between “POM-predicted” and actual measured (*Nereis*) biota-concentration. However, sediments from Smelter A and Smelter E were often among the overestimated by the POM-method (**Figure 10**).



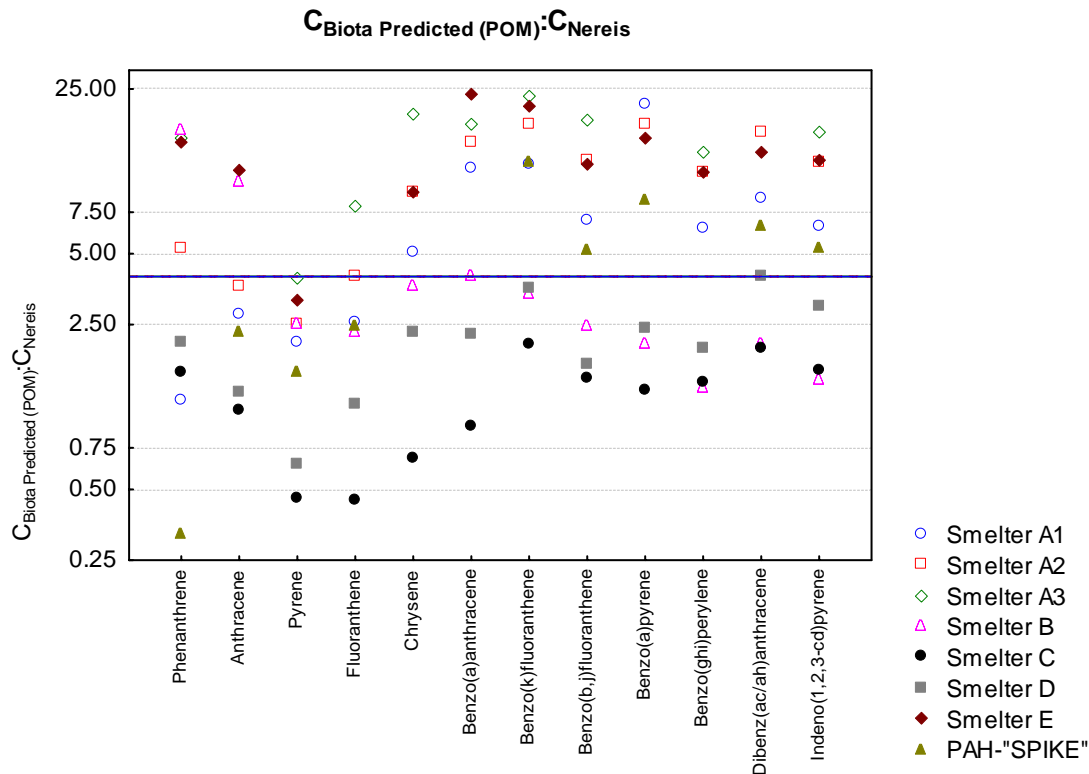


**Figure 10.** The ratio between the “POM-predicted” biota concentrations (predicted from the sediment concentrations, the  $K_{ds}$  (sediment water partitioning coefficients) deduced using POM solid phase extraction, and BCFs (bioconcentration factors)) and the actual measured concentrations in the polychaete *Nereis diversicolor*. The ratio is presented for all sediments and all PAHs (from phenanthrene) presented from left to right with increasing  $K_{ow}$ s. The median (4.0) is presented by a blue line. Note logarithmic scale.

Expected biota concentrations calculated from the Karickhoff et al. (1979) free-energy relationship, sediment concentrations and BCFs corresponded not as good with the concentrations actually measured in *N. diversicolor* (Figure 11). More specific, the expected concentrations were a factor 5 – 3652 (median = 137) higher than the actual accumulated concentrations. The definite highest discrepancies were shown for the Smelter E-sediment, in which the biota concentrations seemed largely overestimated using the Karickhoff et al. (1979) equation, as compared to the concentrations measured in *Nereis diversicolor* (Figure 11).

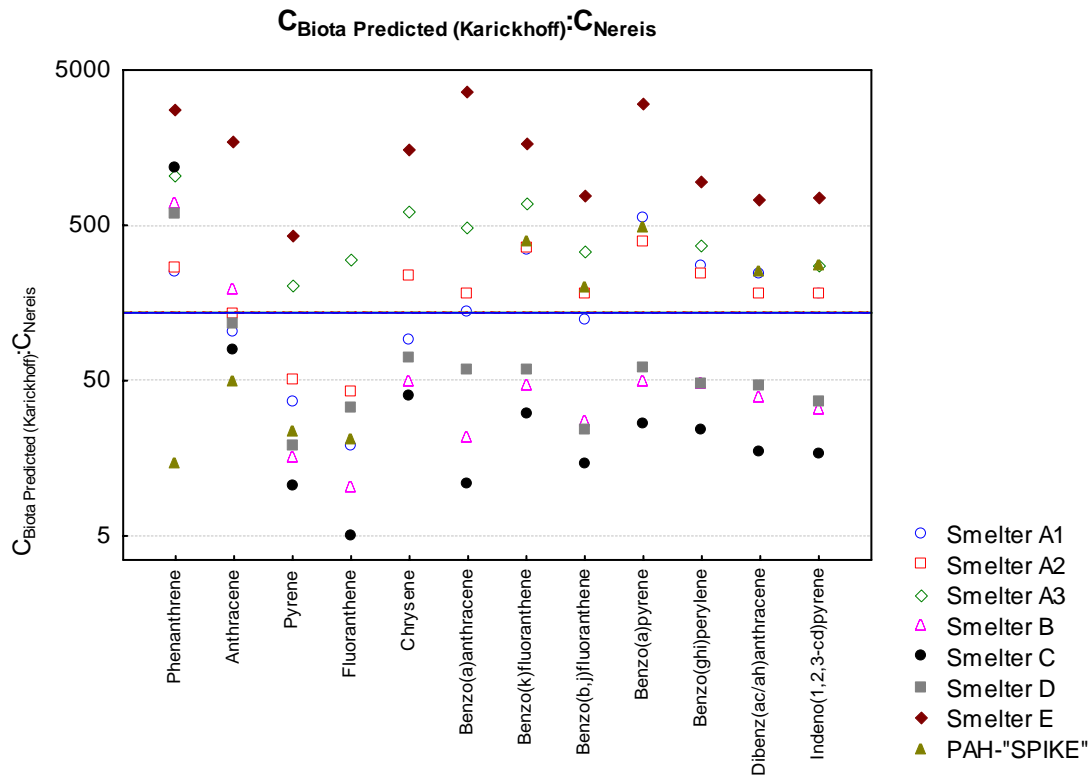


**Figure 11.** The ratio between the “Karickhoff-predicted” biota concentrations (predicted from the sediment concentrations, the  $K_{ds}$  (sediment water partitioning coefficients) deduced using the Karickhoff et al. (1979) free energy relationship, and BCFs (bioconcentration factors)) and the actual measured concentrations in the polychaete *Nereis diversicolor*. The ratio is presented for all sediments and all PAHs (from phenanthrene) presented from left to right with increasing  $K_{ow}$ s. The median (137) is presented by a blue line. Note logarithmic scale.

### 3.2.2 *Hinia reticulata*

Expected biota concentrations calculated from  $K_{ds}$  deduced using POM-SPE, sediment concentrations and bioconcentration factors (BCFs; see pt. *b.* in paragraph 2.7.6 *Calculations*, above) corresponded good with the concentrations actually measured in *H. reticulata*. More specific, the expected concentrations were a factor **0.3 – 32.1** (median = **5.3**) higher than the actual accumulated concentrations (varying with PAH compound and sediment; **Figure 12**). No specific sediment or PAH stands out showing any particular discrepancy between “POM-predicted” and actual measured (*Hinia*) biota-concentration. However, sediments from Smelter A (3) were often among the overestimated, using the POM-method, looking at some of the higher molecular weight PAHs (**Figure 12**).

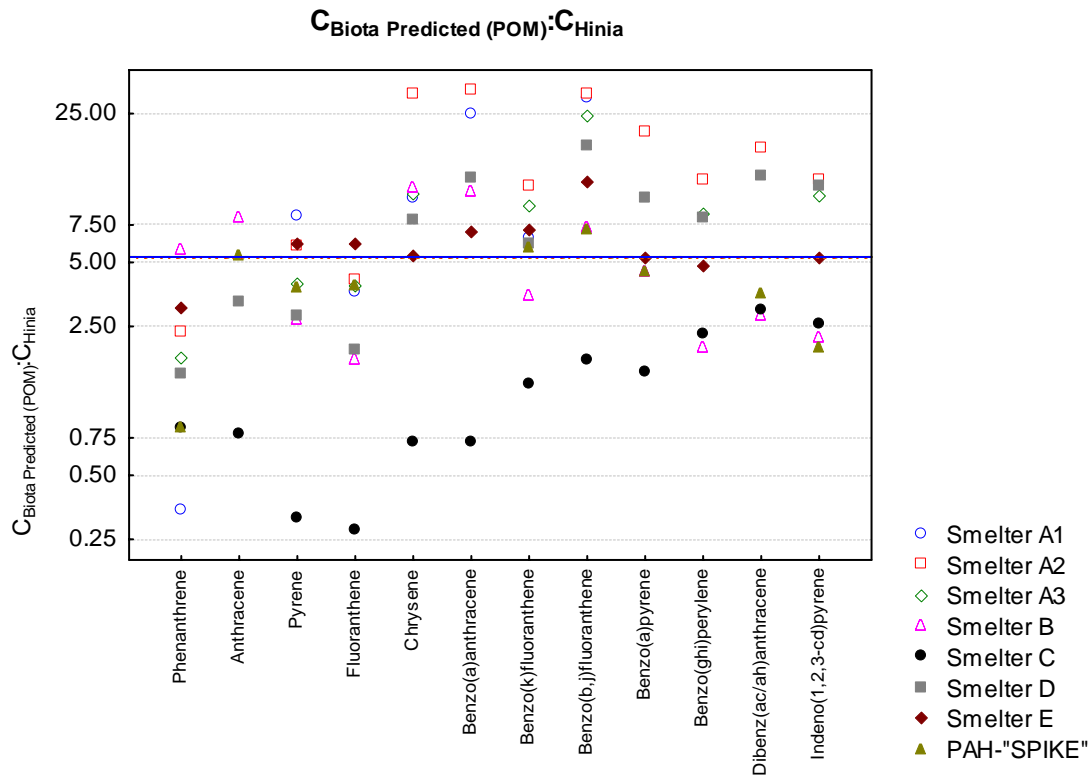


**Figure 12.** The ratio between the “POM-predicted” biota concentrations (predicted from the sediment concentrations, the  $K_{ds}$  (sediment water partitioning coefficients) deduced using POM solid phase extraction, and BCFs (bioconcentration factors)) and the actual measured concentrations in the gastropod *Hinia reticulata*. The ratio is presented for all sediments and all PAHs (from phenanthrene) presented from left to right with increasing  $K_{ow}$ s. The median (5.3) is presented by a blue line. Note logarithmic scale.

Expected biota concentrations calculated from the Karickhoff et al. (1979) free-energy relationship, sediment concentrations and BCFs corresponded not as good with the concentrations actually measured in *H. reticulata* (**Figure 13**). More specific, the expected concentrations were a factor **3.1 – 1057** (median = **152**) higher than the actual accumulated concentrations. The definite highest discrepancies were shown for the Smelter E-sediment, and often Smelter A (2) in which the biota concentrations seemed largely overestimated using the Karickhoff et al. (1979) equation, as compared to the concentrations measured in *Hinia reticulata* (**Figure 13**).

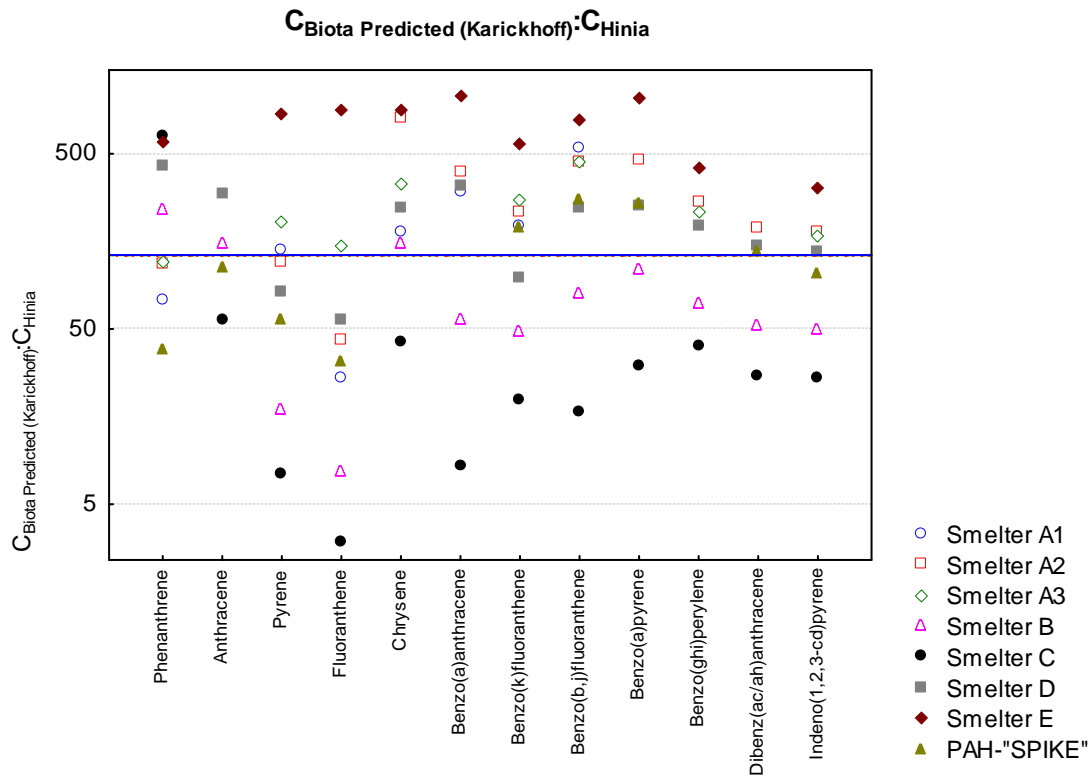


**Figure 13.** The ratio between the “Karickhoff-predicted” biota concentrations (predicted from the sediment concentrations, the  $K_{ds}$  (sediment water partitioning coefficients) deduced using the Karickhoff et al. (1979) free energy relationship, and BCFs (bioconcentration factors)) and the actual measured concentrations in the polychaete *Hinia reticulata*. The ratio is presented for all sediments and all PAHs (from phenanthrene) presented from left to right with increasing  $K_{ow}$ s. The median (152) is presented by a blue line. Note logarithmic scale.

### 3.2.3 *Nuculoma tenuis*

Contrary to the results for *N. diversicolor* and *H. reticulata*, expected biota concentrations calculated from  $K_{ds}$  deduced using POM-SPE, sediment concentrations and bioconcentration factors (BCFs; see pt. b. in paragraph 2.7.6 *Calculations*, above) corresponded not as good with the concentrations actually measured in *N. tenuis* (**Figure 14**). More specific, the expected concentrations were a factor **0.07 – 1.7** (median = **0.17**) higher (in other words, a factor 14 lower to a factor 1.7 higher; median a factor 5.9 lower) than the actual accumulated concentrations (see discussion below).

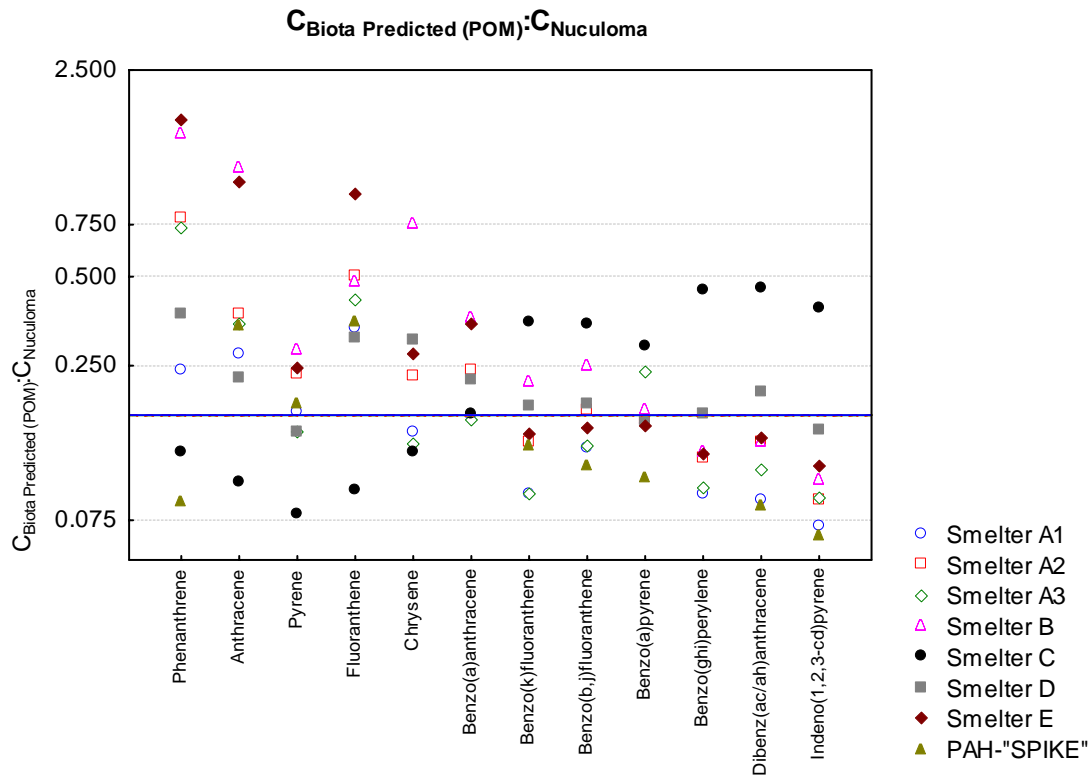


**Figure 14.** The ratio between the “POM-predicted” biota concentrations (predicted from the sediment concentrations, the  $K_{ds}$  (sediment water partitioning coefficients) deduced using POM solid phase extraction, and BCFs (bioconcentration factors)) and the actual measured concentrations in the bivalve *Nuculoma tenuis*. The ratio is presented for all sediments and all PAHs (from phenanthrene) presented from left to right with increasing  $K_{ow}$ s. The median (0.17) is presented by a blue line. Note logarithmic scale.

The expected biota concentrations calculated from the Karickhoff et al. (1979) free-energy relationship, sediment concentrations and BCF corresponded approximately equally good/bad (however, on the conservative side) with the concentrations actually measured in *N. tenuis*, as those calculated by the use of POM-SPE (above; **Figure 15**). More specific, the expected concentrations were a factor **1.1 – 319** (median = **4.2**) higher than the actual accumulated concentrations (see discussion below). The largest discrepancies were shown for the PAHs with the smallest molecular weights in the Smelter E-sediment (**Figure 15**).

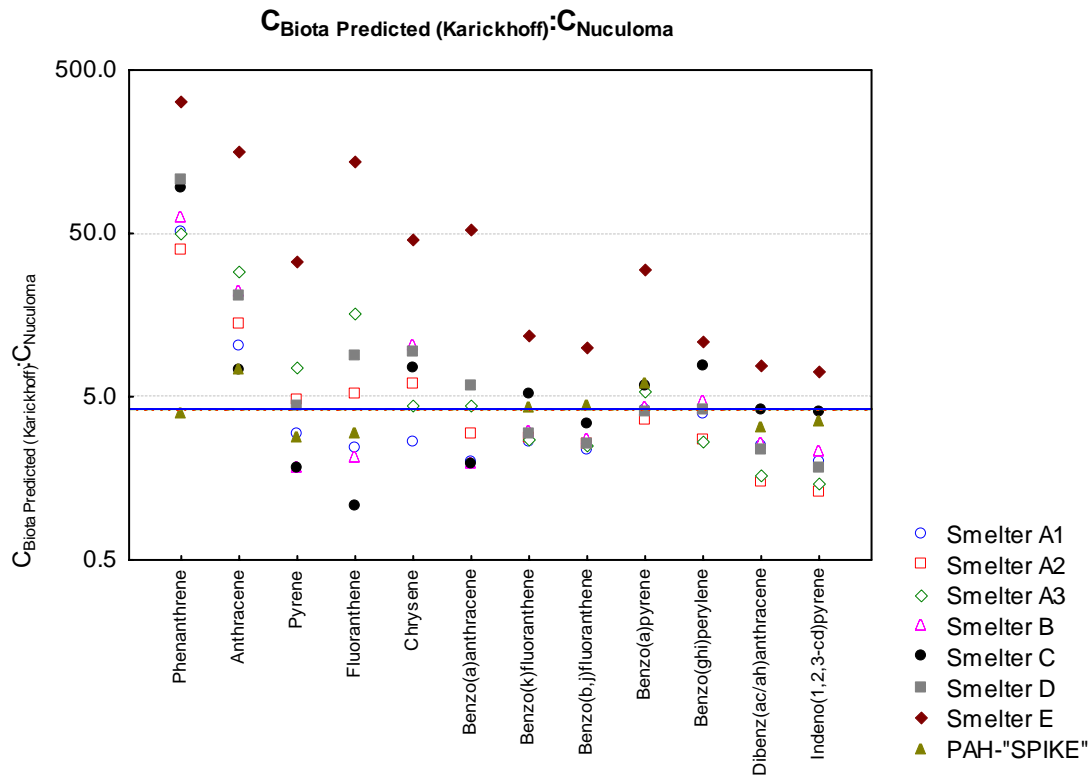


**Figure 15.** The ratio between the “Karickhoff-predicted” biota concentrations (predicted from the sediment concentrations, the  $K_{ds}$  (sediment water partitioning coefficients) deduced using the Karickhoff et al. (1979) free energy relationship, and BCFs (bioconcentration factors)) and the actual measured concentrations in the polychaete *Nuculoma tenuis*. The ratio is presented for all sediments and all PAHs (from phenanthrene) presented from left to right with increasing  $K_{ow}$ s. The median (4.2) is presented by a blue line. Note logarithmic scale.

### 3.3 Biota to sediment accumulation factors (BSAFs)

All individual biota to sediment accumulation factors (BSAFs; predicted using the various methods described above and actual measured BSAFs for all species) are presented in Appendices J-M.

#### 3.3.1 *Nereis diversicolor*

Expected BSAFs calculated from  $K_{ds}$  deduced using POM-SPE, sediment concentrations (OC normalized) and  $K_{ow}$  (see pt. c. in paragraph 2.7.6 Calculations, above) corresponded very good with the BSAFs deduced from the actually measured concentrations in *N. diversicolor* (lipid normalized) and sediments (OC normalized). More specific, the expected BSAFs were a factor **0.08 (0.11** if the PAH-“SPIKE” sediment is excluded) **to 13.8** (median = **1.25**) higher than the actual measured BSAFs (varying with PAH compound and sediment; **Figure 8**). There is some indication that the discrepancy between “POM-predicted” and actual measured (*Nereis*) BSAFs increase with increasing molecular size of the PAHs (**Figure 16**). Sediments from Smelter A (2 and 3) and Smelter E were often among the overestimated by the POM-method (**Figure 16**).

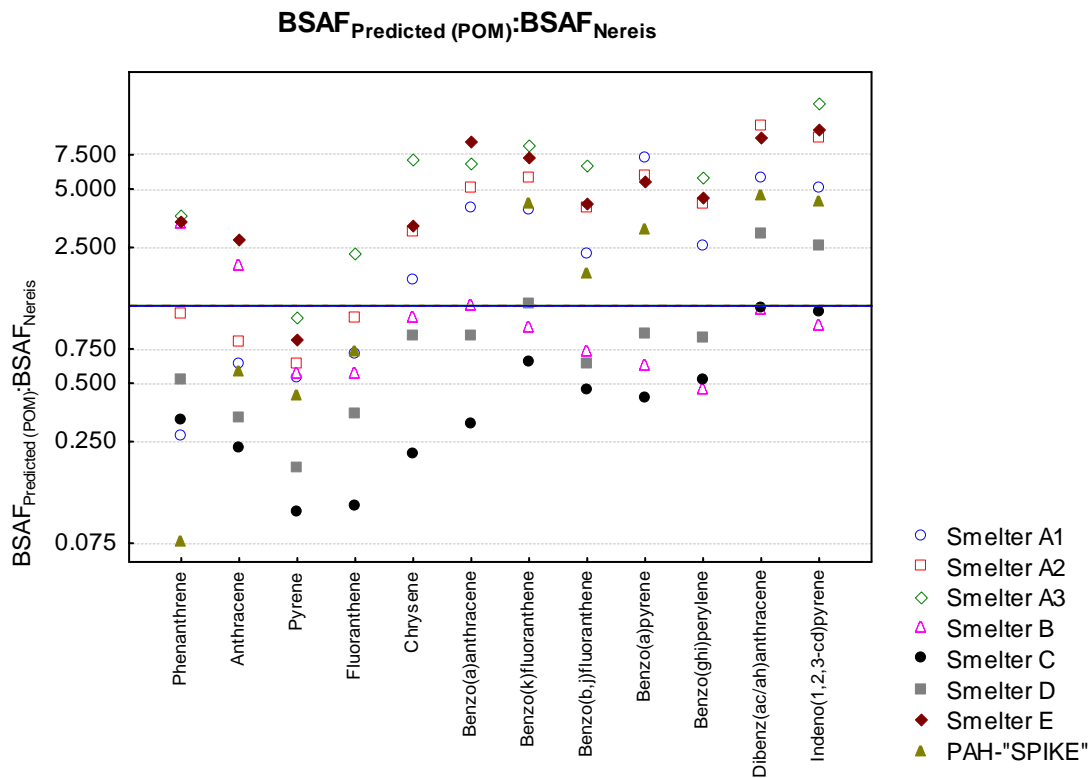


**Figure 16.** The ratio between the “POM-predicted” biota to sediment accumulation factors (calculated from the POM-SPE-deduced  $K_{ds}$  (sediment water partitioning coefficients),  $K_{OWS}$  (the octanol:water partitioning coefficients) and the OC-normalized sediment PAH-concentrations) and the actual measured BSAFs for the polychaete *Nereis diversicolor* (calculated from the lipid normalized concentrations in the organism and the OC-normalized concentrations in the sediments). The ratio is presented for all sediments and all PAHs (from phenanthrene) presented from left to right with increasing  $K_{ow}$ s. The median (1.25) is presented by a blue line. Note logarithmic scale.

Expected BSAFs deduced from the Karickhoff et al. (1979) free-energy relationship ( $BSAF=1.62$ ) corresponded not as good with the BSAFs deduced from the actually measured concentrations in *N. diversicolor* and sediments (**Figure 17**). More specific, the expected BSAFs were a factor **1.3 – 1337** (median = **36.1**) higher than the actual measured BSAFs (**Figure 17**). The definite highest discrepancies were shown for the Smelter E-sediment, in which the BSAFs seemed largely overestimated deduced from the Karickhoff et al. (1979) relationship, as compared to the concentrations measured in *Nereis diversicolor* (**Figure 17**).

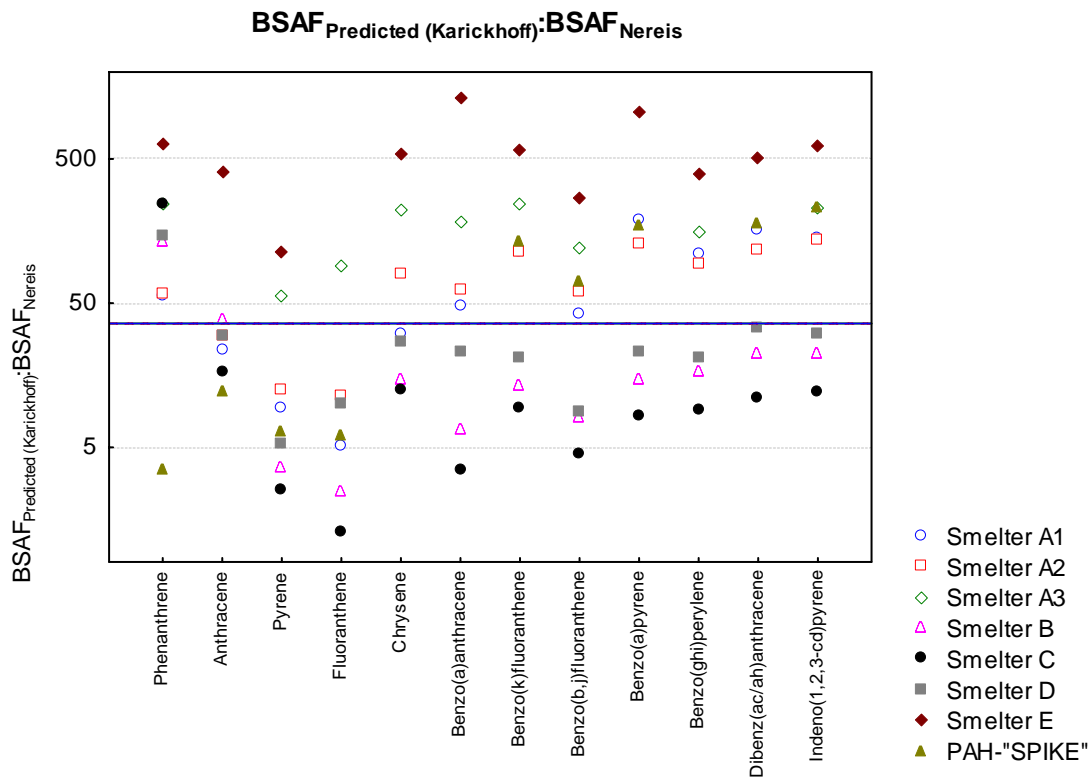


**Figure 17.** The ratio between the “Karickhoff-predicted” biota to sediment accumulation factors ( $\text{BSAF}=1.62$ ), and the actual measured BSAFs for the polychaete *Nereis diversicolor* (calculated from the lipid normalized concentrations in the organism and the OC-normalized concentrations in the sediments). The ratio is presented for all sediments and all PAHs (from phenanthrene) presented from left to right with increasing  $K_{ow}$ s. The median (36.1) is presented by a blue line. Note logarithmic scale.

### 3.3.2 *Hinia reticulata*

Expected BSAFs calculated from  $K_{ds}$  deduced using POM-SPE, sediment concentrations (OC normalized) and  $K_{ow}$  (see pt. c. in paragraph 2.7.6 *Calculations*, above) corresponded very good with the BSAFs deduced from the actually measured concentrations in *H. reticulata* (lipid normalized) and sediments (OC normalized). More specific, the expected BSAFs were a factor **0.03 – 17.3** (median = **1.41**) higher than the actual measured BSAFs (varying with PAH compound and sediment; **Figure 18**). Sediments from Smelter A (2) often showed the highest overestimations of BSAFs, using the POM-method (**Figure 18**). Furthermore, overall the PAHs with larger molecular size (and  $K_{ow}$ ; from chrysene) seemed to be most overestimated.



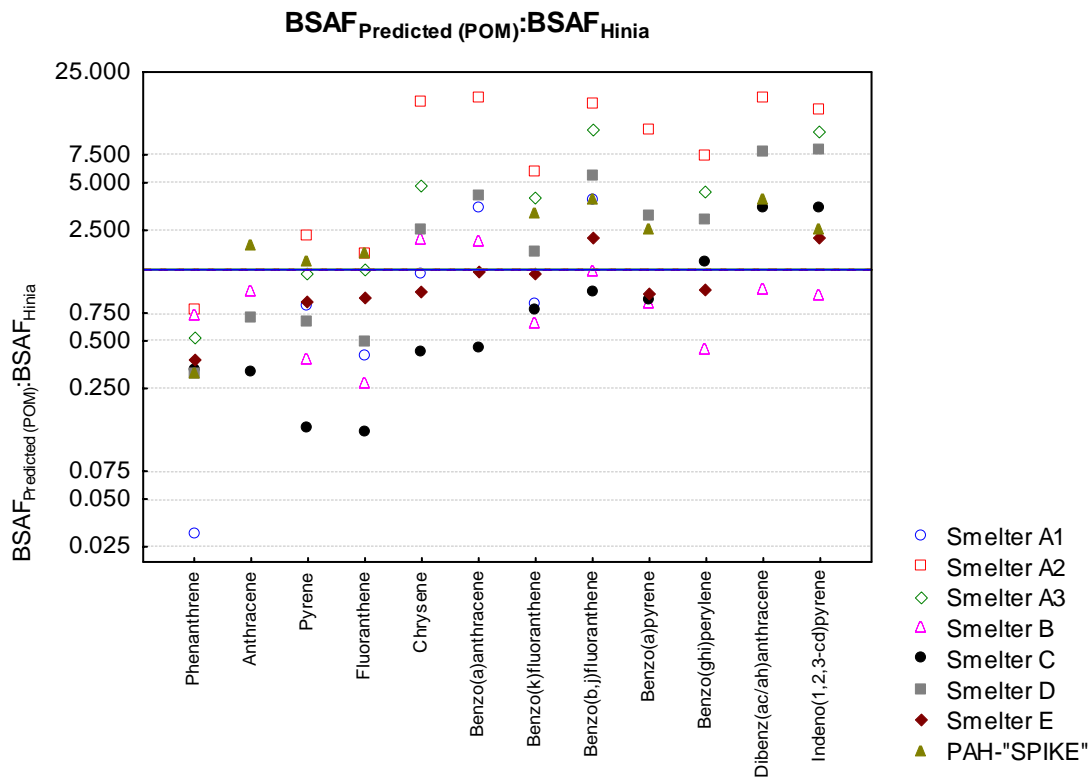


**Figure 18.** The ratio between the “POM-predicted” biota to sediment accumulation factors (calculated from the POM-SPE-deduced  $K_{ds}$  (sediment water partitioning coefficients),  $K_{OWs}$  (the octanol:water partitioning coefficients) and the OC-normalized sediment PAH-concentrations) and the actual measured BSAFs for the gastropod *Hinia reticulata* (calculated from the lipid normalized concentrations in the organism and the OC-normalized concentrations in the sediments). The ratio is presented for all sediments and all PAHs (from phenanthrene) presented from left to right with increasing  $K_{ow}$ s. The median (1.41) is presented by a blue line. Note logarithmic scale.

Expected BSAF deduced from the Karickhoff et al. (1979) free-energy relationship ( $BSAF=1.62$ ) corresponded not as good with the BSAFs deduced from the actually measured concentrations in *H. reticulata* (lipid normalized) and sediments (OC normalized; **Figure 19**). More specific, the expected BSAFs were a factor **1.2 – 419** (median = **47**) higher than the actual measured BSAFs (**Figure 19**). Sediments from Smelter E and Smelter A (2) showed the largest discrepancies, as the BSAFs seemed largely overestimated deduced from the Karickhoff et al. (1979) relationship, as compared to the concentrations measured in *Hinia reticulata* (**Figure 19**).

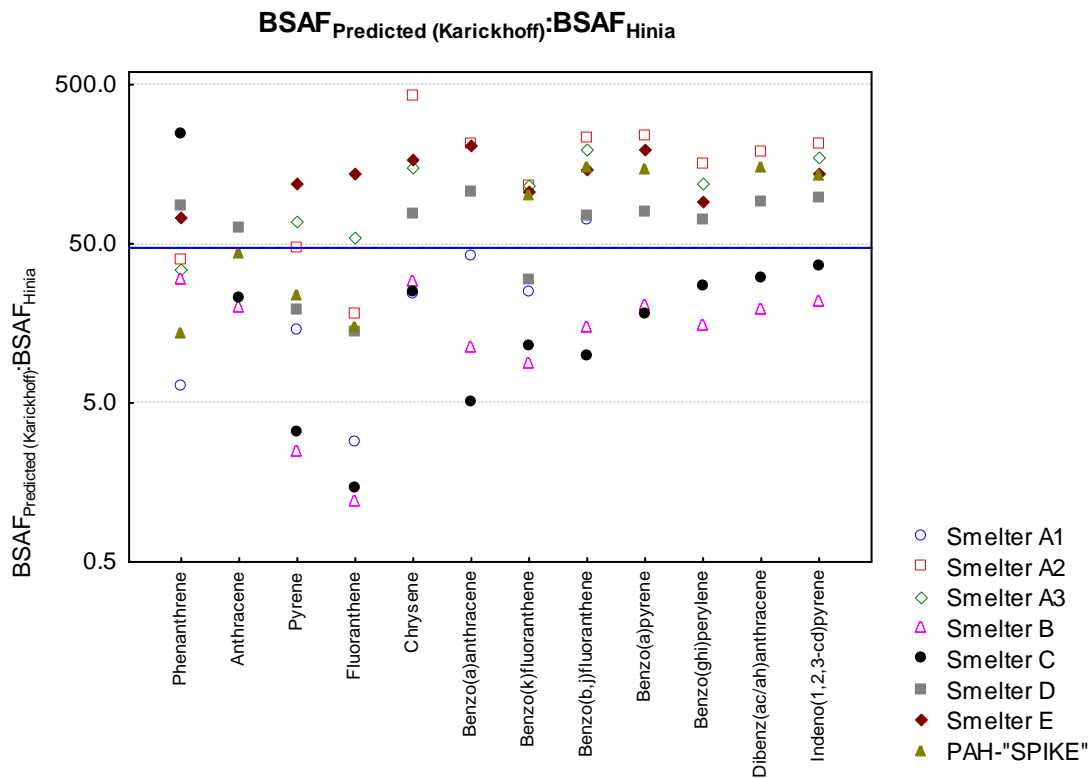


**Figure 19.** The ratio between the “Karickhoff-predicted” biota to sediment accumulation factors ( $BSAF=1.62$ ), and the actual measured BSAFs for the gastropod *Hinia reticulata* (calculated from the lipid normalized concentrations in the organism and the OC-normalized concentrations in the sediments). The ratio is presented for all sediments and all PAHs (from phenanthrene) presented from left to right with increasing  $K_{ow}$ s. The median (47) is presented by a blue line. Note logarithmic scale.

### 3.3.3 *Nuculoma tenuis*

Expected BSAFs calculated from  $K_{ds}$  deduced using POM-SPE, sediment concentrations (OC normalized) and  $K_{ow}$  (see pt. c. in paragraph 2.7.6 *Calculations*, above) corresponded not as good with the BSAFs deduced from the actually measured concentrations in *N. tenuis* (lipid normalized) and sediments (OC normalized), as observed for the other two species *N. diversicolor* and *H. reticulata*. More specific, the expected BSAFs were a factor **0.013 – 0.35** (median = **0.05**) higher (in other words a factor **2.9 – 77** (median = **20**) lower) than the actual measured BSAFs (**Figure 20**; see discussion below).

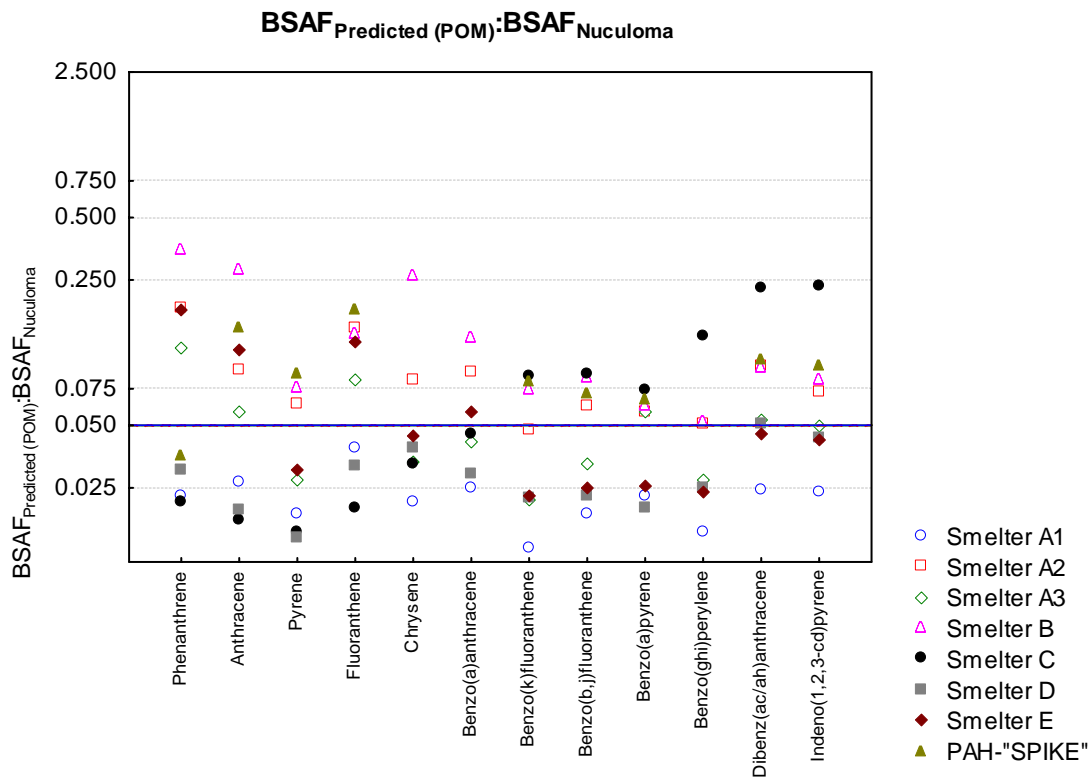


**Figure 20.** The ratio between the “POM-predicted” biota to sediment accumulation factors (calculated from the POM-SPE-deduced  $K_{ds}$  (sediment water partitioning coefficients),  $K_{ows}$  (the octanol:water partitioning coefficients) and the OC-normalized sediment PAH-concentrations) and the actual measured BSAFs for the bivalve *Nuculoma tenuis* (calculated from the lipid normalized concentrations in the organism and the OC-normalized concentrations in the sediments). The ratio is presented for all sediments and all PAHs (from phenanthrene) presented from left to right with increasing  $K_{ow}$ s. The median (0.05) is presented by a blue line. Note logarithmic scale.

Expected BSAF deduced from the Karickhoff et al (1979) free-energy relationship ( $BSAF=1.62$ ) corresponded better with the BSAFs deduced from the actually measured concentrations in *N. tenuis* (lipid normalized) and sediments (OC normalized). More specific, the expected BSAFs were a factor **0.22 – 34.1** (median = **1.29**) higher than the actual measured BSAFs (**Figure 21**). The highest  $BSAF_{Predicted (Karickhoff)}:BSAF_{Measured Nuculoma}$ -ratios were for several PAHs observed for the Smelter E-sediment (**Figure 21**).

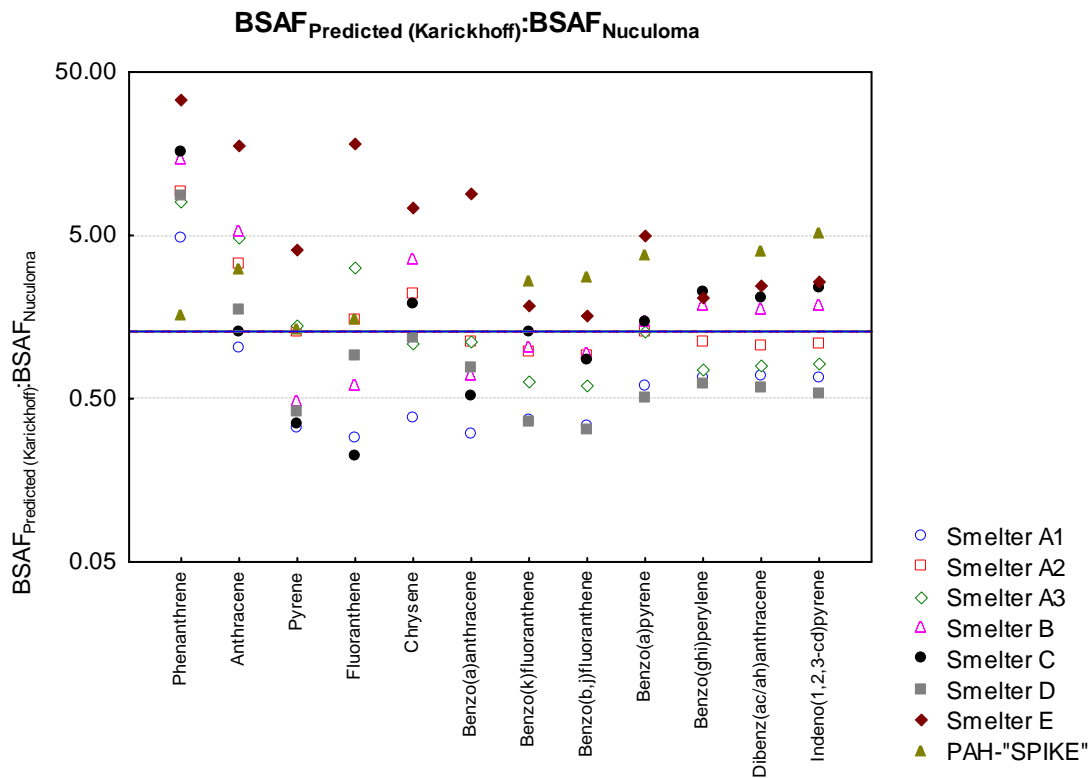


**Figure 21.** The ratio between the “Karickhoff-predicted” biota to sediment accumulation factors ( $BSAF=1.62$ ), and the actual measured BSAFs for the bivalve *Nuculoma tenuis* (calculated from the lipid normalized concentrations in the organism and the OC-normalized concentrations in the sediments). The ratio is presented for all sediments and all PAHs (from phenanthrene) presented from left to right with increasing  $K_{ow}$ s. The median (1.49) is presented by a blue line. Note logarithmic scale.

### 3.4 PAH-profiles

The divergencies between the results for *Nuculoma tenuis* and the other two species, *Nereis diversicolor* and *Hinia reticulata*, gave reason for further scrutiny (see discussion below). The PAH-profiles (relative concentrations; the proportion each PAH compound to the sum of all compounds) was calculated in each of the matrices (whole sediment, pore water (deduced using the POM-SPE method) and the three organisms). This profile is plotted for the Smelter A1 sediment in **Figure 22**.

The pattern shows that the bivalve *Nuculoma tenuis* displays a similar PAH-profile as the whole sediment (**Figure 22**). The polychaet *Nereis diversicolor* and the gastropod *Hinia reticulata* show profiles more similar to the sediment pore water (**Figure 22**).

The relative concentrations of the PAHs in all matrices from all sediments were subjected to a Principal Component Analysis (PCA; **Figure 23**). The PCA also showed that the PAH profile in *Nereis diversicolor* and *Hinia reticulata* resembled the PAH profile in pore water (located more to the right in the score plot: **Figure 23 b**), while the profile in *Nuculoma tenuis* resembled more the PAH profile in whole sediment (located more to the left in the score plot: **Figure 23 b**). Higher proportions of the compounds fluoranthene, pyrene, anthracene and phenanthrene was important for segregating the pore water PAH-profile from the whole sediment PAH-profile (loading positively on principal component 1, explaining 52 % of the variance in the material; **Figure 23 a**).

The PCA also showed that the sediment spiked with PAH, pore water from this sediment, and all three species exposed to this sediment showed PAH-profiles different from the other sediments, pore water from these sediments, and organisms exposed to them (**Figure 23**). This is shown by the PAH-“SPIKE” data points placed to the lower right in the score plot (**Figure 23 b**), due to higher relative concentrations of phenanthrene and anthracene (**Figure 23 a**). Therefore, the PCA was performed again, without the PAH-“SPIKE” sediment, pore water from this sediment or organisms exposed to it (**Figure 24**). This analysis also showed the strongest resemblance between the PAH-profiles in whole sediment and *Nuculoma tenuis*.

**Smelter A1**

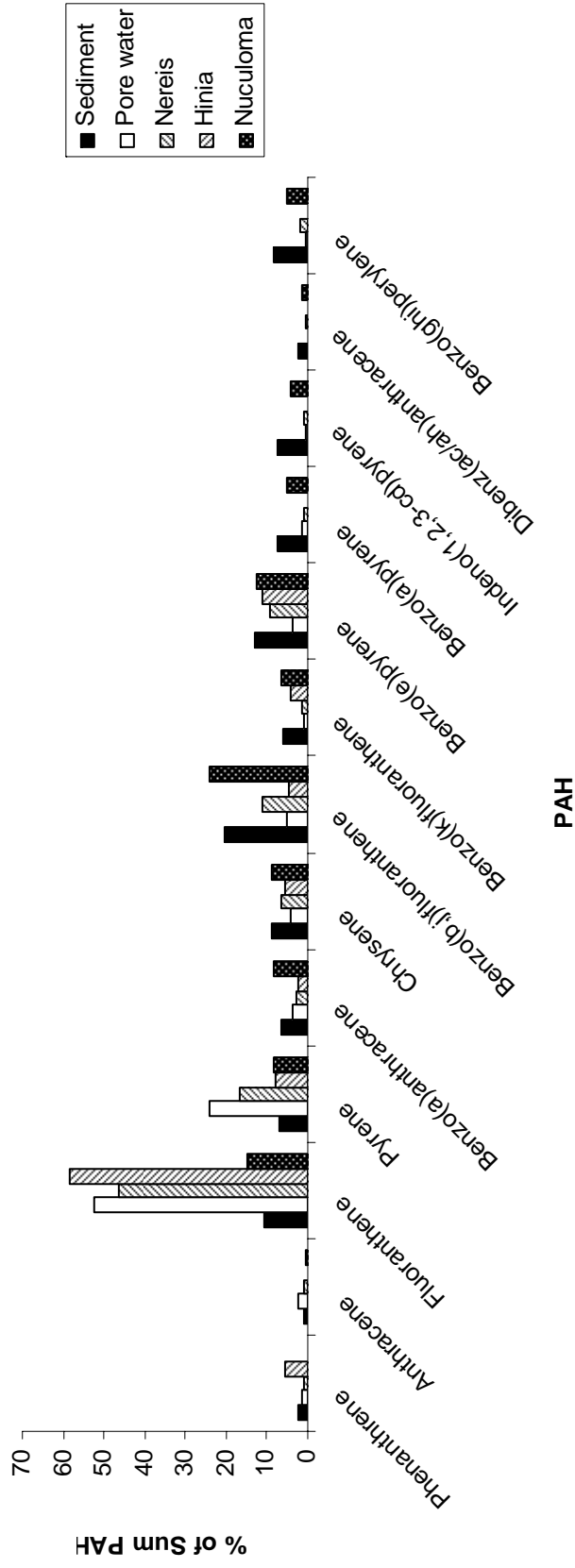
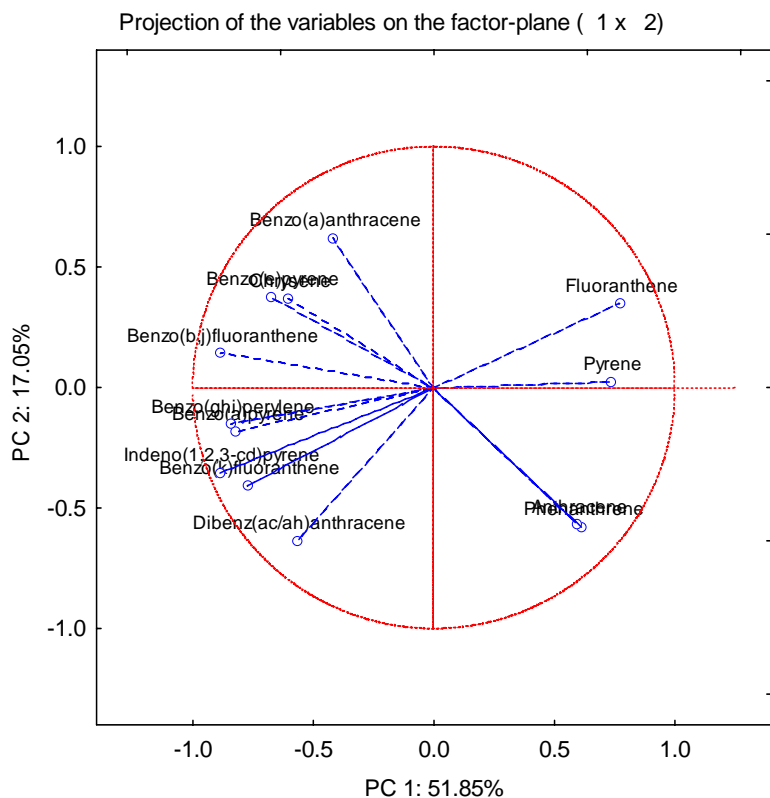


**Figure 22.** Relative concentrations of individual PAH compounds (expressed as sum of all compounds; sum-PAH) in whole sediment from Smelter A1, pore water from this sediment (measured by POM-SPE) and *Nereis diversicolor*, *Hinia reticulata* and *Nuculoma tenuis* exposed to the Vefsnefjord 1 sediment for 4 weeks.

a.



b.

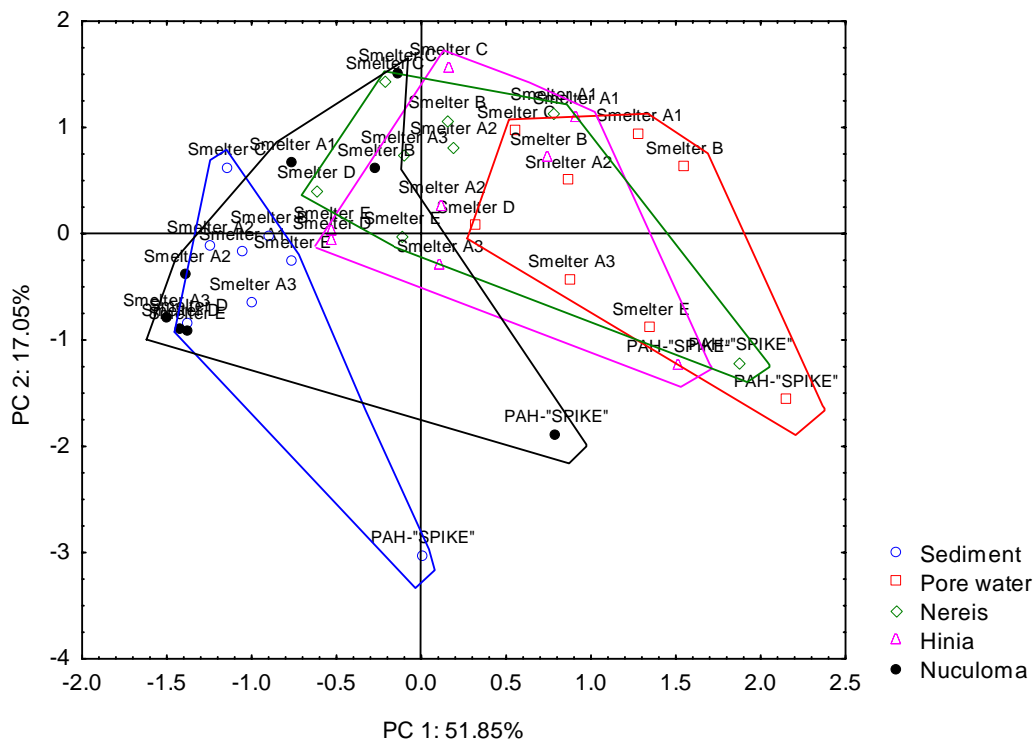
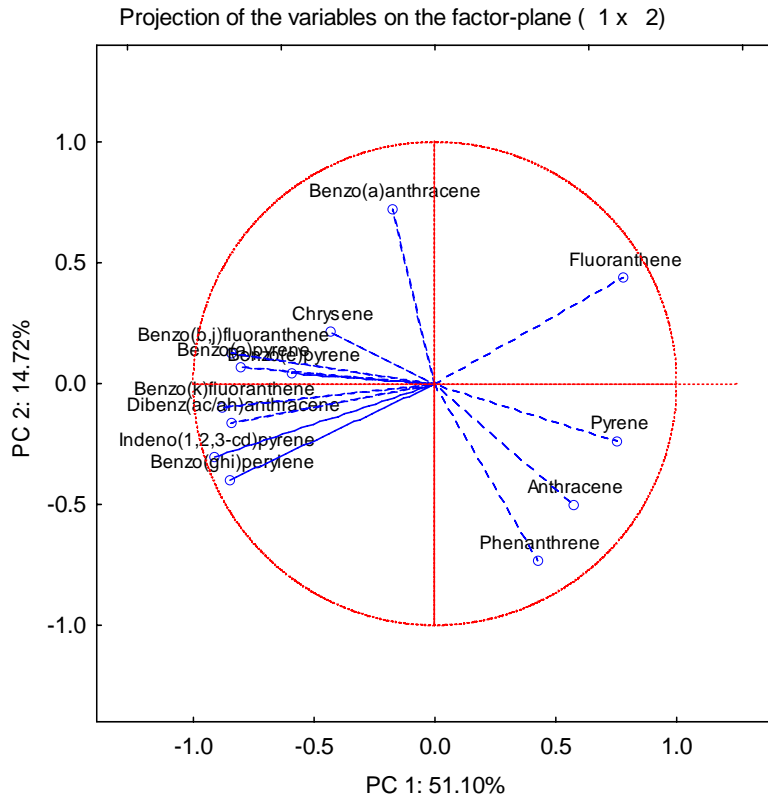


**Figure 23.** Loading- (a.) and score-plot (b.) for a Principal Component Analysis (PCA) performed on relative concentrations (% of sum-PAH) in whole sediment, sediment porewater, *Nereis diversicolor*, *Hinia reticulata* and *Nuculoma tenuis* (all groups/sediments included).

a.



b.

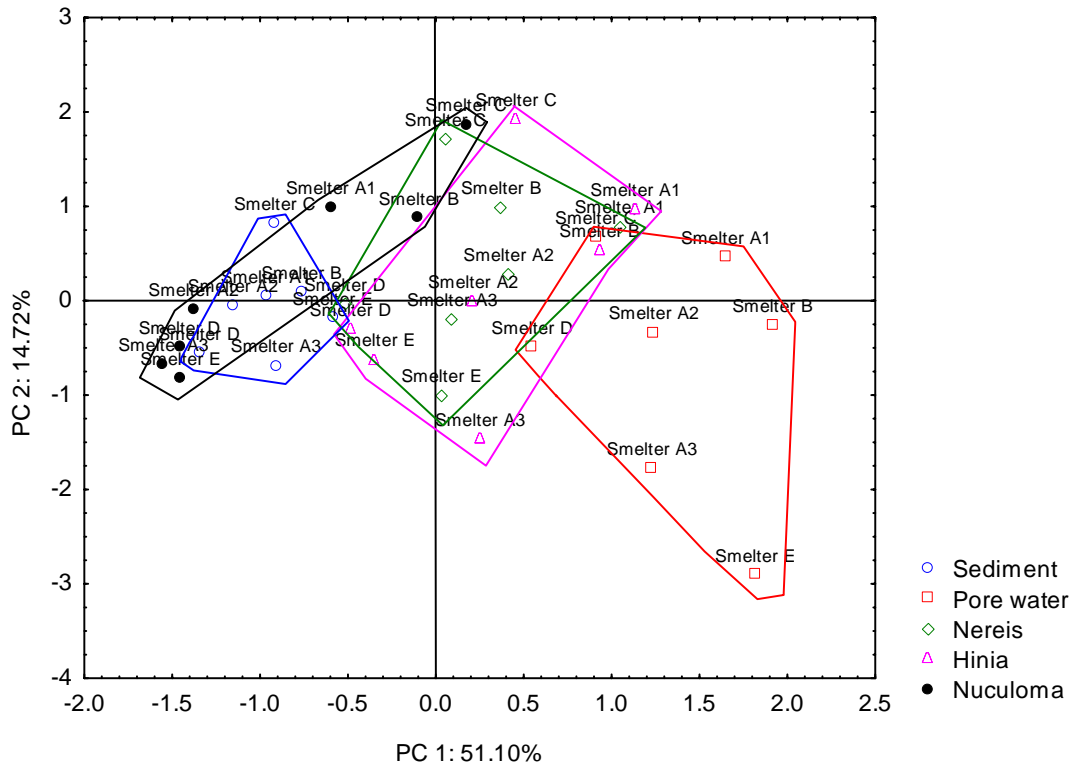


**Figure 24.** Loading- (a.) and score-plot (b.) for a Principal Component Analysis (PCA) performed on relative concentrations (% of sum-PAH) in whole sediment, sediment porewater, *Nereis diversicolor*, *Hinia reticulata* and *Nuculoma tenuis* (all groups/sediments, except PAH-“SPIKE” included).



## 4. Discussion

The results from the POM experiments showed that the PAHs associated with the sediments in the vicinity of the smelters were stronger adsorbed/absorbed to the particles than the Karickhoff et al. (1979) free energy relationship implies. This further implies that the bioavailable fraction is correspondingly lower, and one would expect lower bioaccumulated concentrations. It was, however, difficult to show any good relationships between the total organic carbon or black carbon content in the sediments and the sediment:water partitioning coefficients ( $K_d$ ), plotted for each PAH compound.

The accumulated concentrations measured in *Nereis diversicolor* and *Hinia reticulata* were in fact very similar to biota concentrations expected based on the POM-deduced sediment-water partitioning coefficients ( $K_{ds}$ ). Thus, the measured biota to sediment accumulation factors (BSAFs) agreed also very well with those expected from the POM-deduced  $K_{ds}$ .

On the other hand, this good correspondence was not observed for the third species, *Nuculoma tenuis*. PAH concentrations measured in *N. tenuis* were up to two orders of magnitude (a factor >300) higher than the concentrations measured in *Nereis diversicolor* and *Hinia reticulata*. In fact, for some compounds and sediments, the *Nuculoma* wet weight concentrations were even higher than the sediment dry weight concentrations.

Due to the low biomass obtained from the *N. tenuis* individuals, no replicates from each of the sediments could be analysed. Still, only 0.35 to 0.61 g of mussel soft tissue was obtained per sample for analysis. Thus, the risk of contamination of the biological tissue samples by contaminated particles is higher than for the other species (for which 1.5 - 6 g of tissue was obtained per individual sample for analysis). Assuming that the PAHs in the sediment are associated with organic material, approximately only 1% (weight:weight; equivalent to approximately 5 mg) of sediment organic material in a *Nuculoma* sample would increase its concentration from those observed in *Nereis* and *Hinia* to the concentrations actually measured in the *Nuculoma* samples.

As most protobranchs, *Nuculoma tenuis* is a selective deposit feeder. During feeding, its tentacles are extended into the bottom sediments. Deposited materials adhere to the mucus-covered surface of the tentacles and then are transported by cilia back to the palps, which function as sorting devices (Barnes, 1987). It is likely that PAH-contaminated deposit material in the stomach may have been analysed as part of the organism. Furthermore, when the organisms sort the particles, light particles are carried by crest cilia to the mouth, while heavy particles are carried by groove cilia to the palp margins, where they are ejected into the mantle cavity (Barnes, 1987).

The reason for suspecting contamination of *Nuculoma* samples by particulate material in the first place, arise from differences observed in the different PAH profiles (relative concentrations expressed as percentages of sum PAH) in the different sample matrices. As expected, the profiles in the *Nereis* and *Hinia* samples resemble the profiles in pore water (measured by POM-SPE). Fluoranthene and pyrene are e.g. two compounds that are measured in high concentrations in pore water relative to the other (and higher molecular weight) PAHs (i.e. they have lower  $K_{ds}$ ). The relative concentrations of these compounds are lower in sediment samples and *Nuculoma* samples. On the other hand, the higher molecular PAHs, such as benzo(*b,j*)fluoranthene, benzo(*a*)pyrene, indeno(*1,2,3-cd*)pyrene and benzo(*ghi*)perylene constitute higher percentages of sum PAH in sediment samples and *Nuculoma* samples, while they are low or not detected in pore water, *Nereis* and *Hinia* (**Figure 22**).

One the other hand, one could explain the higher concentrations of PAHs in *Nuculoma* with a lower capability of metabolising and eliminating the compounds, than *N. diversicolor* and *H. reticulata*. It is

likely that especially *Nereis* has a higher capability of biotransformation than *Nuculoma*, which is a primitive protobranch. The question that still remains is whether the rate of metabolism is sufficient to alter the equilibrium appreciable. Studying several organisms, Rust et al. (2004b) found high rates of metabolism of benzo(a)pyrene in the polychaetes *Nereis virens* and *Nereis succinea*, and that bioaccumulation factors were inversely related to the capability of metabolizing benzo(a)pyrene.

Metabolites of pyrene have earlier been shown in *Nereis diversicolor* (Christensen et al. 2002; Giessing et al. 2003), however, pyrene was one of the compounds that bioaccumulated the most in *Nereis* and also *Hinia* (as expected from the pore water concentrations). Metabolism of e.g. benzo(b,j)fluoranthene is less likely, still this compound does not bioaccumulate as much as pyrene in *Nereis* and *Hinia*, even though the concentration in sediment is higher than the concentration of pyrene. The concentration of benzo(b,j)fluoranthene in porewater, however, is lower than the pyrene concentrations. Therefore, it seems that the bioavailable compounds in sediment pore water may be more important than metabolic capability for determining the bioaccumulation. Benzo(b,j)-fluoranthene constitutes high percentages of sum PAH in *Nuculoma* (higher than pyrene), as it does in the sediment samples.

It therefore seems likely that uncontrollable factors, rendering us uncertain of the contamination by particulate matter in the *Nuculoma* samples, may have caused the pattern observed in this species, which deviates from the patterns observed in *Nereis* and *Hinia*. It would seem less likely that a selective higher uptake of the higher molecular weight (and thus stronger particle adsorbed) PAHs would occur in *Nuculoma*. It would seem correspondingly unlikely that the pattern observed in *Nereis* and *Hinia* should be a result of a higher capability than *Nuculoma* to metabolise and eliminate especially the higher molecular weight PAHs, that are hardly detectable in pore water (high  $K_{ds}$ ) and are therefore less bioavailable. However, the many uncertainties associated with *Nuculoma tenuis* render the interpretations somewhat inconclusive for this species, and further investigations would be necessary to eliminate these uncertainties.

## 4.1 Conclusions

The results from the POM-experiments showed that the PAHs associated with the sediments in the vicinity of the smelters were stronger (a median factor of at least a magnitude) adsorbed/absorbed to the particles than the Karickhoff et al. (1979) free energy relationship implies. This further implies that the bioavailable fraction is correspondingly lower, and one would expect lower bioaccumulated concentrations. The accumulated concentrations measured in *Nereis diversicolor* and *Hinia reticulata* were in fact very similar to biota concentrations expected based on the POM-deduced sediment-water partitioning coefficients ( $K_{ds}$ ). Thus, the measured biota to sediment accumulation factors (BSAFs) agreed also very well with those expected from the POM-deduced  $K_{ds}$ .

On the other hand, this good correspondence was not observed for the third species, *Nuculoma tenuis*. There were however logistical intractabilities connected to this species biology and size that render it probable that particulate sedimentary matter contaminated the *Nuculoma* tissues analyses. Exceptionally high PAH concentrations relative to the other two organisms and a PAH profile more similar to that of the sediments support this assumption. However, the many uncertainties associated with this species, render the interpretations somewhat inconclusive, and further investigations would be necessary to eliminate the uncertainties for this species.

## 5. References

- Barnes RD. 1987. Invertebrate zoology. 5<sup>th</sup> ed. 893 pp. Harcourt Brace Jovancovich Inc. Orlando FL.
- Breedveld GD., Bakke T., Eek E., Helland A., Källqvist T., and A. Oen. 2005. Risk assessment of contaminated sediments – Guidance manual. SFT-report TA-no. 2085/2005 (In Norwegian).
- Christensen M., Andersen O., and GT. Banta. 2002. Metabolism of pyrene by the polychaetes *Nereis diversicolor* and *Arenicola marina*. *Aquat. Toxicol.* 58:15-25.
- Cornelissen G., Gustafsson Ö. 2004. Sorption to environmental black carbon in sediment with and without organic carbon and native sorbates. *Environ. Sci. Technol.*, 38;148-155.
- Cornelissen G., Gustafsson Ö., Bucheli TD., Jonker MTO., Koelmans AA., and PCM. Noort. 2005. Extensive sorption of organic compound to black carbon, coal, and kerogen in sediments and soils: Mechanisms and consequences for distribution, bioaccumulation, and biodegradation. *Environ. Sci. Technol.*, 39:6881-6895
- Cornelissen G., Breedveld G., Kalaitzidis S., Christanis K., Kibsgaard A. and AMP. Oen. 2006. Strong sorption of native PAHs to pyrogenic and unburned carbonaceous geosorbents in sediments. *Environ. Sci. Technol.*, 40:1197-1203.
- Fowler SW., Polikarpow, GG., Elder, DL., Parsi, P., and JP. Villeneuve. 1978. Polychlorinated biphenyls: accumulation from contaminated sediments and water by the polychaete *Nereis diversicolor*. *Mar. Biol.* 48:303-309.
- Giessing AMB., Mayer LM., and TL. Forbes. 2003. 1-Hydroxypyrene glucuronide as the major aqueous pyrene metabolite in tissue and gut fluid from the marine deposit feeding polychaete *Nereis diversicolor*. *Environ. Toxicol. Chem.* 22:1107-1114.
- Goerke H., 1984. Testing the fate of xenobiotics in *Nereis diversicolor* and *Nereis virens* (Polychaeta). In: Persoone, G., Jaspers, E., Claus, C. (eds), Ecotoxicological testing for the marine environment, University Gent/IZWO, Gent, pp. 53-66.
- Gosling E. 2003. Bivalve molluscs – Biology, Ecology and Culture. Fishing News Bookd, Blackwell Publishing, Oxford, UK. 443 pp.
- Hylland K. 1996. Bioaccumulation of contaminants from marine sediments – Establishment of a test system. NIVA-report 3537. (In Norwegian).
- Jonker MTO. and AA. Koelmans. 2001. Polyoxymethylene solid phase extraction as a partitioning method for hydrophobic organic chemicals in sediments and soot. *Environ. Sci. Technol.*, 35:3742-3748.
- Karickhoff SW., Brown DS. and TA. Scott. 1979. Sorption of hydrophobic pollutants on natural sediments. *Wat. Res.*, 13:241-248.
- Khalil MF., Ghosh U. and JP. Kreitinger. 2006. Role of weathered coal tar pitch in the partitioning of polycyclic aromatic hydrocarbons in manufactured gas plant site sediments. *Environ. Sci. Technol.*, 40:5681-5687.
- Krumbein WC., and FJ. Pettijohn. 1938. Manual of sedimentary petrography. Mather, K.F. (Ed), Appelton-Century-Crofts, New York, 549 pp.
- Lee H., Boese BL., Pelletier J., Winsor M., Specht DT., and RC. Randall. 1991. Guidance manual: bedded sediment bioaccumulation tests. EPA/600/x-89/302.

- Næs K. 1998. The distribution and effects on Norwegian fjord and coastal ecosystems of polycyclic aromatic hydrocarbons (PAHs) generated by the production of primary aluminium and manganese alloys. Thesis for the degree of Doctor Philosophiae.
- Næs K., Axelman J., Broman D. and C. Näf. 1998. Role of soot carbon and other carbon matrices in the distribution of PAHs among particles, DOC and the dissolved phase in the effluent and recipient waters of an aluminium reduction plant. *Environ. Sci. Technol.*, 32: 1786-1792.
- Rust AJ., Burgess RM., McElroy AE., Cantwell MG. and BJ. Brownawell. 2004a. Influence of soot carbon on the bioaccumulation of sediment-bound polycyclic aromatic hydrocarbons by marine benthic invertebrates: An interspecies comparison. *Environ. Toxicol. Chem.*, 23:2594-3603.
- Rust AJ., Burgess RM., Brownawell BJ., and AE. McElroy. 2004b. Relationship between metabolism and bioaccumulation of benzo[a]pyrene in benthic invertebrates. *Environ. Toxicol. Chem.*, 23:2587-2593.
- Ruus A., Schaanning M., Øxnevad S. and K. Hylland. 2005. Experimental results on bioaccumulation of metals and organic contaminants from marine sediments. *Aquat. Toxicol.* 72: 273-292.

## 6. Appendices

- Appendix A** Concentrations of PAHs, and other variables in sediments
- Appendix B** Concentrations of PAHs and lipid content in *Nereis diversicolor*
- Appendix C** Concentrations of PAHs and lipid content in *Hinia reticulata*
- Appendix D** Concentrations of PAHs and lipid content in *Nuculoma tenuis*
- Appendix E** Sediment:water partitioning coefficients ( $K_d$ ) determined by POM-SPE
- Appendix F** Organic carbon:water partitioning coefficients ( $K_{OC}$ )
- Appendix G** Bioconcentration factors (BCFs)
- Appendix H** Predicted biotaconcentrations deduced *i.a.* using POM-SPE
- Appendix I** Predicted biotaconcentrations deduced *i.a.* from Karickhoff et al. (1979)
- Appendix J** Biota to sediment accumulation factors (BSAFs) measured for *Nereis diversicolor*
- Appendix K** Biota to sediment accumulation factors (BSAFs) measured for *Hinia reticulata*
- Appendix L** Biota to sediment accumulation factors (BSAFs) measured for *Nuculoma tenuis*
- Appendix M** Predicted biota to sediment accumulation factors (BSAFs)

## Appendix A.

Concentrations ( $\mu\text{g}/\text{kg}$  dry wt) of PAHs (sum PAH is sum-PAH<sub>EPA 16</sub>), Total dry matter (TDM, %), proportion of particles smaller than  $63 \mu\text{m}$  (%), total organic carbon (%) and amount black carbon (%) in the different sediments.

	Naphthalene	Acenaphthylene	Acenaphthene	Fluorene	Dibenzofluorene	Phenanthrene	Anthracene	Fluoranthene	Pyrene	Benzo(a)anthracene
Smelter A1	2.3	<2	14	8.2	5.6	80	28	380	250	230
Smelter A2	11	<2	29	19	12	190	69	610	470	510
Smelter A3	16	<2	38	22	13	200	44	350	310	200
Smelter B	1600	50	2100	1600	890	14000	2800	35000	32000	22000
Smelter C	2900	130	3700	2700	1400	22000	8700	56000	38000	61000
Smelter D	27	2.2	110	53	33	520	140	1300	1200	950
Smelter E	140	2.8	320	180	90	1300	260	2100	1800	1300
PAH-"SPIKE"	10	<2	16	18	15	550	320	720	510	49
Control	2.4	<2	<2	<2	<2	3.3	<2	6.3	5.5	2.2

	Chrysene	Benzo(b)fluoranthene	Benzo(k)fluoranthene	Benzo(e)pyrene	Benzo(a)pyrene	Perylene	Indeno(1,2,3-cd)pyrene	Dibenz(a,h)anthracene	Benzo(g,h,i)perylene	Sum PAH
Smelter A1	310	730	220	460	270	68	260	82	300	3164.5
Smelter A2	1100	1800	520	1200	570	150	720	210	840	7668
Smelter A3	270	610	200	400	270	68	340	89	390	3349
Smelter B	33000	66000	18000	44000	30000	5900	23000	6700	24000	311850
Smelter C	140000	150000	44000	95000	72000	14000	42000	12000	39000	694130
Smelter D	1400	3900	1300	2400	2200	550	1900	520	2200	17722.2
Smelter E	1700	2600	910	1500	1600	400	1300	360	1300	17172.8
PAH-"SPIKE"	44	340	340	37	250	26	220	200	37	3624
Control	4.8	7.2	2.1	5	3.1	5.6	3.3	<2	2.2	42.4

	TDM (%)	<63 $\mu\text{m}$ (%)	TOC (%)	BC (%)
Smelter A1	62.5	56	1.24	0.11
Smelter A2	66.62	76	1.19	0.15
Smelter A3	44.21	96	1.59	0.1
Smelter B	57.74	72	6.76	5.77
Smelter C	51.52	76	5.46	1.87
Smelter D	67.83	30	1.32	0.22
Smelter E	63.77	75	1.36	0.43
PAH-"SPIKE"	73.74	82	0.63	<0.1
Control	76.62	84	0.42	<0.1

## Appendix B.

Concentrations ( $\mu\text{g/kg}$  wet wt) of PAHs (sum PAH is sum-PAH<sub>EPA 16</sub>) and lipid content (%) in the polychaete *Nereis diversicolor* exposed to the different sediments.

	Naphthalene	Acenaphthylene	Acenaphthene	Fluorene	Dibenzofluorene	Phenanthrene	Anthracene	Fluoranthene	Pyrene	Benzo(a)anthracene
Smelter A1 1	<6	<0.5	<0.5	0.76	1.2	1.7	2.4	120	50	13
Smelter A1 2	<6	<0.5	0.62	0.84	1.1	1.7	1.3	79	30	5.7
Smelter A1 3	6.8	<0.5	0.94	0.54	0.98	2.3	1.4	88	32	5.6
Smelter A2 1	<6	<0.5	0.65	0.77	0.69	3.8	3	66	45	8
Smelter A2 2	<6	<0.5	<0.5	0.73	0.64	4	2.4	63	43	10
Smelter A2 3	20	0.56	<0.5	<0.5	0.65	4.9	2.8	81	58	18
Smelter A3 1	<6	<0.5	0.52	<0.5	<0.5	<1	<0.5	<3	5.4	1.1
Smelter A3 2	<6	<0.5	0.64	<0.5	<0.5	1.1	<0.5	4.3	8.2	1.1
Smelter A3 3	<6	<0.5	<0.5	<0.5	<0.5	0.81	<0.5	3.9	5.6	<0.5
Smelter B 1	<6	0.63	3.4	1.6	1.3	20	14	2500	1600	710
Smelter B 2	12	0.61	4.9	1.1	1.4	23	15	2700	1700	640
Smelter B 3	16	0.93	4.2	0.53	1.2	20	13	2700	1700	600
Smelter C 1	<6	<0.5	130	3.6	1.5	23	130	11000	3800	4300
Smelter C 2	7.9	2.1	120	2.3	14	25	160	14000	4200	6100
Smelter C 3	<6	2	110	2.1	7.5	13	80	11000	2700	4400
Smelter D 1	<6	<0.5	1.4	1.1	1.1	3.5	6.5	150	250	40
Smelter D 2	<6	<0.5	1.4	1.3	0.97	4.4	5.3	160	280	51
Smelter D 3	7.4	<0.5	2.5	0.95	1.1	5.6	5.8	180	330	53
Smelter E 1	<6	<0.5	1.2	0.76	<0.5	2.2	0.59	<3	15	1.1
Smelter E 2	<6	<0.5	1.5	0.87	<0.5	3.3	0.87	7.4	20	2.1
Smelter E 3	<6	<0.5	1.4	<0.5	<0.5	2.3	0.72	<4	18	<1.5
PAH- "SPIKE" 1	<6	<0.5	7.2	5.4	11	400	93	250	160	<0.5
PAH- "SPIKE" 2	16	0.61	6.1	2	9.3	410	62	300	200	<1.5
PAH- "SPIKE" 3	<6	0.67	8.6	3.6	8.7	370	66	330	220	<1.5
Control 1	<6	<0.5	<0.5	<0.5	<0.5	<1	<0.5	<3	<1.5	<0.5
Control 2	<6	<0.5	<0.5	<0.5	<0.5	0.72	<0.5	<0.6	<0.9	<0.5
Control 3	14	<0.5	<0.5	<0.5	<0.5	<0.8	<0.5	<4	<2	<1.5

**MEDIANS:**

	Naphthalene	Acenaphthylene	Acenaphthene	Fluorene	Dibenzofluorene	Phenanthrene	Anthracene	Fluoranthene	Pyrene	Benzo(a)anthracene
Smelter A1	0	0	0.62	0.76	1.1	1.7	1.4	88	32	5.7
Smelter A2	0	0	0	0.73	0.65	4	2.8	66	45	10
Smelter A3	0	0	0.52	0	0	0.81	0	3.9	5.6	1.1
Smelter B	12	0.63	4.2	1.1	1.3	20	14	2700	1700	640
Smelter C	0	2	120	2.3	14	23	130	11000	3800	4400
Smelter D	0	0	1.4	1.1	1.1	4.4	5.8	160	280	51
Smelter E	0	0	1.4	0.76	0	2.3	0.72	0	18	1.1
PAH- "SPIKE"	0	0.61	7.2	3.6	9.3	400	66	300	200	0
Control	0	0	0	0	0	0	0	0	0	0

Cont. on next page

	Chrysene	Benzo( <i>b</i> )fluoranthene	Benzo( <i>k</i> )fluoranthene	Benzo( <i>e</i> )pyrene	Benzo( <i>a</i> )pyrene	Perylene	Indeno(1,2,3- <i>cd</i> )pyrene	Dibenz( <i>ac</i> / <i>ab</i> )anthracene	Benzo( <i>ghi</i> )perylene	Sum PAH
Smelter A1 1	12	35	5	32	4.5	1.1	3.6	1.4	5.6	254.96
Smelter A1 2	11	17	2.1	1.7	1.7	<0.5	2.2	0.56	3.3	157.02
Smelter A1 3	12	21	2.3	1.8	<1.3	<0.7	1.8	0.61	2.8	178.09
Smelter A2 1	13	35	3.6	3.8	4.7	1.7	5.5	2.2	11	202.22
Smelter A2 2	17	37	5.5	3.7	5.3	1.7	6.4	2.2	11	207.53
Smelter A2 3	32	58	12	53	8	4	11	4.1	24	334.36
Smelter A3 1	1.2	5	0.91	5.2	0.78	<0.5	1.6	<0.5	2.6	19.11
Smelter A3 2	1.7	5.7	0.83	5.7	<0.5	<0.5	1.5	<0.5	2.5	27.57
Smelter A3 3	1.1	2.7	<0.5	3.9	<0.5	<0.5	0.78	<0.5	2.3	17.19
Smelter B1	240	1800	290	1400	450	93	240	69	320	8258.63
Smelter B 2	500	1600	250	1300	390	79	180	56	280	8352.61
Smelter B 3	430	1500	260	1200	290	54	200	58	280	8072.66
Smelter C 1	4200	6000	660	4100	1600	400	760	220	870	33696.6
Smelter C 2	2800	9900	1200	6400	2700	560	1100	340	1300	43957.3
Smelter C 3	1900	8500	1200	5300	2200	480	880	280	1100	34367.1
Smelter D 1	49	320	45	300	84	35	62	16	100	1128.5
Smelter D 2	75	550	77	480	120	34	76	19	130	1550.4
Smelter D 3	65	570	91	510	130	39	89	23	150	1703.25
Smelter E 1	1.3	9.2	1.8	8.4	1.7	<0.5	2.4	0.81	3.6	41.66
Smelter E 2	5.2	14	2.9	12	2.9	0.67	3.8	1.2	5.5	71.54
Smelter E 3	3.6	11	1.6	9	<1.3	<0.7	2.1	0.72	3.8	45.24
PAH- "SPIKE" 1	<0.5	12	5.7	1.4	3.6	<0.5	2.4	2.3	2.4	944
PAH- "SPIKE" 2	<1	12	6.3	<3	1.8	<0.7	1.8	2.8	<0.5	1021.41
PAH- "SPIKE" 3	<1	19	14	<3	4.1	<0.7	3.2	3.4	<0.5	1042.57
Control 1	<0.5	<0.5	<0.5	<0.5	<0.5	<0.5	<0.5	<0.5	<0.5	0
Control 2	<0.5	<1.5	<0.5	<1	<0.5	<0.5	<0.5	<0.5	<0.5	0.72
Control 3	<1	<3.2	<0.5	<3	<1.3	<0.7	<0.5	<0.5	<0.5	14

**MEDIANS:**

	Chrysene	Benzo( <i>b</i> )fluoranthene	Benzo( <i>k</i> )fluoranthene	Benzo( <i>e</i> )pyrene	Benzo( <i>a</i> )pyrene	Perylene	Indeno(1,2,3- <i>cd</i> )pyrene	Dibenz( <i>ac</i> / <i>ab</i> )anthracene	Benzo( <i>ghi</i> )perylene	Sum PAH
Smelter A1	12	21	2.3	18	1.7	0	2.2	0.61	3.3	178.09
Smelter A2	17	37	5.5	38	5.3	1.7	6.4	2.2	11	207.53
Smelter A3	1.2	5	0.83	5.2	0	0	1.5	0	2.5	19.11
Smelter B	430	1600	260	1300	390	79	200	58	280	8258.63
Smelter C	2800	8500	1200	5300	2200	480	880	280	1100	34367.1
Smelter D	65	550	77	480	120	35	76	19	130	1550.4
Smelter E	3.6	11	1.8	9	1.7	0	2.4	0.81	3.8	45.24
PAH-"SPIKE"	0	12	6.3	0	3.6	0	2.4	2.8	0	1021.41
Control	0	0	0	0	0	0	0	0	0	0.72

**Lipid (%)**

Smelter A1	0.91
Smelter A2	0.89
Smelter A3	0.98
Smelter B	0.8
Smelter C	0.85
Smelter D	1.01
Smelter E	0.95
PAH-"SPIKE"	0.97
Control	0.91



# Appendix C.

Concentrations (µg/kg wet wt) of PAHs (sum PAH is sum-PAH<sub>EPA 16</sub>) and lipid content (%) in the gastropod *Hinia reticulata* exposed to the different sediments.

	Naphthalene	Acenaphthylene	Acenaphthene	Fluorene	Dibenzofluorene	Phenanthrene	Anthracene	Fluoranthene	Pyrene	Benzo(a)anthracene
Smelter A1 1	110	<2	<2	<2	<2	7.4	<2	62	8.8	<2
Smelter A1 2	59	<2	2	<2	<2	5.9	<2	39	7.4	2.6
Smelter A1 3	<17	<2	<2	<2	<2	<3	<2	76	8.2	2.7
Smelter A2 1	94	<2	2.4	2.1	<2	10	2.6	64	20	4.7
Smelter A2 2	79	<2	<2	<2	<2	9.1	<2	46	12	4.6
Smelter A2 3	630	<2	<2	<2	<2	6.8	<2	74	19	4.4
Smelter A3 1	130	<2	<2	<2	<2	6.7	<2	5.2	4.4	<2
Smelter A3 2	m	m	m	m	m	m	m	18	11	3
Smelter A3 3	100	<2	<2	4	<2	7.4	<2	7.9	5.6	<2
Smelter B 1	m	m	m	m	m	m	m	4100	2300	240
Smelter B 2	31	<2	12	8	4.9	75	21	3600	1500	240
Smelter B 3	<17	<2	5.4	4.1	2.6	42	14	2800	1600	200
Smelter C 1	m	m	m	m	m	m	m	17000	5100	5500
Smelter C 2	32	<2	37	4.6	24	43	180	19000	5800	5800
Smelter C 3	m	m	m	m	m	m	m	m	m	m
Smelter D 1	m	m	m	m	m	m	m	95	58	7.6
Smelter D 2	28	<2	<2	<2	<2	7.3	2.5	140	88	9.2
Smelter D 3	<17	<2	<2	<2	<2	5.1	2.1	94	64	12
Smelter E 1	110	<2	<2	<2	<2	13	<2	9.4	9.2	3.8
Smelter E 2	45	<2	2.4	<2	<2	11	<2	16	15	6.5
Smelter E 3	<17	<2	<2	<2	<2	5.2	<2	4.3	5.4	2.9
PAH- "SPIKE" 1	m	m	m	m	m	m	m	240	110	4.5
PAH- "SPIKE" 2	<17	<2	<2	<2	<2	140	22	150	68	<2
PAH- "SPIKE" 3	<17	<2	<2	<2	<2	170	36	190	83	<2
Control 1	100	<2	<2	<2	<2	8.5	<2	2.6	2.2	<2
Control 2	76	<2	<2	3.2	18	7.6	<2	3.7	2.3	<2
Control 3	<17	<2	<2	<2	<2	3.4	<2	<4	<3	<2

**MEDIANS:**

	Naphthalene	Acenaphthylene	Acenaphthene	Fluorene	Dibenzofluorene	Phenanthrene	Anthracene	Fluoranthene	Pyrene	Benzo(a)anthracene
Smelter A1	59	0	0	0	0	5.9	0	62	8.2	2.6
Smelter A2	94	0	0	0	0	9.1	0	64	19	4.6
Smelter A3	115	0	0	2	0	7.05	0	7.9	5.6	0
Smelter B	15.5	0	8.7	6.05	3.75	58.5	17.5	3600	1600	240
Smelter C	32	0	37	4.6	24	43	180	18000	5450	5650
Smelter D	14	0	0	0	0	6.2	2.3	95	64	9.2
Smelter E	45	0	0	0	0	11	0	9.4	9.2	3.8
PAH-"SPIKE"	0	0	0	0	0	155	29	190	83	0
Control	76	0	0	0	0	7.6	0	2.6	2.2	0

Cont. on next page

	Chrysene	Benzo(b <sub>f</sub> )fluoranthene	Benzo(k)fluoranthene	Benzo(e)pyrene	Benzo(a)pyrene	Perylene	Indeno(1,2,3-cd)pyrene	Dibenz(ac/ah)anthracene	Benzo(g/h <i>i</i> )perylene	Sum PAH
Smelter A1 1	5.1	4.2	2.9	10	<2	<2	<2	<2	<2	200.4
Smelter A1 2	6.1	6.4	4.4	14	2.5	3.3	2.2	<2	3.1	140.6
Smelter A1 3	6.6	4.9	4.2	12	<2	<2	<2	<2	<2	102.6
Smelter A2 1	6.1	15	1.1	36	4.9	<2	6.4	2.1	8.7	254
Smelter A2 2	5	16	8.5	33	4.6	<2	6.7	2.3	10	203.8
Smelter A2 3	4.2	12	6.9	33	4.4	2.5	4.2	<2	1.3	778.9
Smelter A3 1	2.2	3.6	2.1	5.7	<2	<2	2.1	<2	3.1	159.4
Smelter A3 2	3.9	7.1	4.7	9.9	3.4	<2	5.1	<2	6.4	62.6
Smelter A3 3	2.2	3.8	2.1	5.8	<2	<2	2.4	<2	4	139.4
Smelter B1	110	550	250	940	180	37	100	42	190	8062
Smelter B2	220	670	310	930	260	56	200	64	260	7471
Smelter B3	140	470	190	600	160	130	130	43	160	5958.5
Smelter C1	2800	7200	1900	5400	1800	370	510	180	650	42640
Smelter C2	2500	7300	1800	5400	2000	420	600	190	710	45996.6
Smelter C3	m	m	m	m	m	m	m	m	m	m
Smelter D1	s16	48	45	130	27	8.1	18	5.9	32	336.5
Smelter D2	s19	53	46	140	31	12	23	4.7	29	461.7
Smelter D3	s19	56	56	130	29	9.2	20	7.2	40	374.4
Smelter E1	s6.1	11	5.3	14	5	<2	5.5	<2	8	180.2
Smelter E2	s7.8	15	8.7	22	8	2.4	8.7	<2	10	146.3
Smelter E3	s4.1	9.8	5.1	14	4.2	<2	5.7	<2	8.7	51.3
PAH- "SPIKE" 1	s3.4	12	13	8.7	7.2	2.1	6.4	5.8	6.7	405.6
PAH- "SPIKE" 2	<2	3.9	10	<2	4	<2	3.3	3.9	<2	405.1
PAH- "SPIKE" 3	<2	8.7	14	3.5	6.7	<2	6.8	5.2	3.2	523.6
Control 1	<2	<2	<2	<2	<2	<2	<2	<2	<2	113.3
Control 2	<2	<2	<2	<2	<2	<2	<2	<2	<2	92.8
Control 3	<2	<2	<2	<2	<2	<2	<2	<2	<2	3.4

**MEDIANS:**

	Chrysene	Benzo(b <sub>f</sub> )fluoranthene	Benzo(k)fluoranthene	Benzo(e)pyrene	Benzo(a)pyrene	Perylene	Indeno(1,2,3-cd)pyrene	Dibenz(ac/ah)anthracene	Benzo(g/h <i>i</i> )perylene	Sum PAH
Smelter A1	6.1	4.9	4.2	12	0	0	0	0	0	140.6
Smelter A2	5	15	8.5	33	4.6	0	6.4	2.1	10	254
Smelter A3	2.2	3.8	2.1	5.8	0	0	2.4	0	4	139.4
Smelter B	140	550	250	930	180	37	130	43	190	7471
Smelter C	2650	7250	1850	5400	1900	395	555	185	680	44318.3
Smelter D	19	53	45	130	29	9.2	20	5.9	32	393.4
Smelter E	6.1	11	5.3	14	5	0	5.7	0	8.7	154.1
PAH-"SPIKE"	0	8.7	13	3.5	6.7	0	6.4	5.2	3.2	409
Control	0	0	0	0	0	0	0	0	0	92.8

**Lipid (%)**

Smelter A1	0.36
Smelter A2	1.4
Smelter A3	1.2
Smelter B	0.51
Smelter C	1.6
Smelter D	0.84
Smelter E	0.51
PAH-"SPIKE"	1.5
Control	0.74

## Appendix D.

Concentrations ( $\mu\text{g}/\text{kg}$  wet wt) of PAHs (sum PAH is sum-PAH<sub>EPA 16</sub>) and lipid content (%) in the bivalve *nuculoma tenuis* exposed to the different sediments.

	Naphthalene	Acenaphthylene	Acenaphthene	Fluorene	Dibenzotiofophene	Phenanthrene	Anthracene	Fluoranthene	Pyrene	Benzo(a)anthracene
Smelter A1	<120	<2.5	2.2	<2.6	2.5	8.4	14	680	390	390
Smelter A2	<120	2.6	2.1	<2.6	2.1	27	27	530	480	610
Smelter A3	<120	<2.5	3	2.8	1.1	17	6.1	74	150	120
Smelter B	<120	2.8	27	21	15	220	120	13000	15000	7100
Smelter C	<120	4.7	160	32	95	280	1400	52000	22000	24000
Smelter D	<120	3.2	5.3	3.1	<0.8	25	33	590	1200	520
Smelter E	<120	<2.5	5.2	3.2	1.4	20	7.8	60	230	76
PAH-"SPIKE"	<120	3.5	11	12	16	1500	450	2100	1700	29
Control	<120	3.4	2.2	<2.6	<0.8	<5	1.2	<3.8	4.6	<1.5

Cont. on next page

	Chrysene	Benzo(b,j)fluoranthene	Benzo(k)fluoranthene	Benzo(e)pyrene	Benzo(a)pyrene	Perylene	Indeno(1,2,3-cd)pyrene	Dibenz(ac/ah)anthracene	Benzo(ghi)perylene	Sum PAH
Smelter A1	410	1100	300	570	230	44	200	60	230	4014.6
Smelter A2	670	2600	710	1500	580	130	890	260	990	8378.7
Smelter A3	170	690	210	410	140	19	280	76	350	2288.9
Smelter B	2100	16000	4000	9300	4600	730	2800	870	2900	68760.8
Smelter C	15000	36000	7100	20000	10000	1700	3600	1200	3500	176276.7
Smelter D	490	5100	1500	2700	1800	360	1500	370	1500	14639.6
Smelter E	120	850	260	500	170	34	260	76	330	2468.2
PAH-"SPIKE"	27	540	570	62	290	26	190	220	69	7711.5
Control	<1.6	7.4	2.1	7.2	<1.3	<5	5.3	<2.1	13	39.2

	Lipid (%)
Smelter A1	0.39
Smelter A2	0.97
Smelter A3	0.66
Smelter B	0.94
Smelter C	0.69
Smelter D	0.34
Smelter E	0.44
PAH-"SPIKE"	1.7
Control	0.3

## Appendix E.

Sediment: water partitioning coefficients ( $K_d$ ; L/kg), determined by POM-SPE (triplicates and medians).

	Naphthalene	Acenaphthylene	Acenaphthene	Fluorene	Dibenzotiofene	Phenanthrene	Anthracene	Fluoranthene	Pyrene	Benzo(a)anthracene
Smelter A1 1				25350		11381		8377	11417	56157
Smelter A1 2				95011		16302		9249	13880	91997
Smelter A1 3				12707		12884		12020	14189	72856
Smelter A2 1				13696		11543		11449	14133	71079
Smelter A2 2				24539		20668		16724	17296	96711
Smelter A2 3				49529		48107		59597	42045	194353
Smelter A3 1				22136		33535		59658	49418	219831
Smelter A3 2				24538		39257		61755	47606	215341
Smelter A3 3				63589		37812		28915	24029	178994
Smelter B 1				110294		42229		32084	27832	195395
Smelter B 2				40848		32487		29324	25598	143636
Smelter B 3				748844		81388		38775	46613	217747
Smelter C 1				934558		127756		59133	88061	403392
Smelter C 2				1391437		116263		60331	74858	314249
Smelter C 3				85722		35507		53732	26045	172812
Smelter D 1				37277		28456		35516	22831	173470
Smelter D 2				1164294		41364		37382	20823	141471
Smelter D 3				55391		60707		193501	108358	1043915
Smelter E 1				58583		54720		166173	90017	891086
Smelter E 2				518229		188111		579595	193986	2962240
Smelter E 3				4359		2652		3804	4056	320688
PAH- "SPIKE" 1				7972		3933		5152	5542	386278
PAH- "SPIKE" 2				6464		5010		7264	7885	798442
PAH- "SPIKE" 3										
Control 1										
Control 2										
Control 3									19912	

Cont. on next page

	Chrysene	Benzo( <i>b,j</i> )fluoranthene	Benzo( <i>k</i> )fluoranthene	Benzo( <i>e</i> )pyrene	Benzo( <i>a</i> )pyrene	Perylene	Indeno(1,2,3- <i>cd</i> )pyrene	Dibenz( <i>ac/ah</i> )anthracene	Benzo( <i>ghi</i> )perylene
Smelter A1 1	73151	112426	130970	97741	205252	396088	524662	396088	357342
Smelter A1 2	103692	249645	444550	204699	336266	970854	1101100	970854	730614
Smelter A1 3	123925	141522	190861	110879	226092	213264	486238	213264	267481
Smelter A2 2	110903	120609	158426	110052	158308	256020	354750	256020	261296
Smelter A2 3	158295	149964	195423	134616	219493	313064	413261	313064	290147
Smelter A3 1	178839	210772	353548	223610	293372	626389	873308	594700	594700
Smelter A3 2	201641	237531	369191	213078	270989	450010	608233	416240	416240
Smelter A3 3	201252	283584	372203	216294	406631	462772	612604	446682	446682
Smelter B 1	362410	600362	738761	572083	1346157	2427022	3723871	2427022	2476866
Smelter B 2	408833	654986	985812	648799	1503575	2667381	3566701	2667381	2531254
Smelter B 3	146814	457110	524843	436363	999333	1417907	2123147	1417907	1518004
Smelter C 1	738324	308469	426090	287762	692844	723622	1229792	723622	735104
Smelter C 2	1305116	432344	631691	363728	902505	946590	1321449	946590	958255
Smelter C 3	1276031	437137	680249	366762	918354	1199016	1700517	1199016	1181294
Smelter D 1	176442	157386	171276	137946	273618	332889	397997	332889	343880
Smelter D 2	161065	149670	172947	131966	283254	273888	328775	273888	283233
Smelter D 3	146186	140528	162323	126885	276853	299687	373933	299687	330352
Smelter E 1	901713	713877	862303	548341	2199152	1448692	1959675	1448692	1197896
Smelter E 2	764173	561596	656904	432820	1861446	1108480	1458952	1108480	961872
Smelter E 3	3058523	1468805	1759388	1049973	4843142	2764221	3511778	2764221	2079310
PAH- "SPIKE" 1	276077	175883	153534	695899	244271	472484	775487	472484	
PAH- "SPIKE" 2	353402	197441	159908	866367	298987	384302	781906	384302	
PAH- "SPIKE" 3	716072	380724	333124		595517	1112569	1908266	1112569	
Control 1									
Control 2									
Control 3									

Cont. on next page

**MEDIANS:**

	Naphthalene	Acenaphthylene	Acenaphthene	Fluorene	Dibenzofluorene	Phenanthrene	Anthracene	Fluoranthene	Pyrene	Benzo(a)anthracene
Smelter A1			60181			13841	8813	12648		74077
Smelter A2			13696			12884	12020	14189		72856
Smelter A3			24538			39257	59658	47606		215341
Smelter B			63589			37812	29324	25598		178994
Smelter C			934558			116263	59133	74858		314249
Smelter D			85722			35507	37382	22831		172812
Smelter E			58583			60707	193501	108358		1043915
PAH-"SPIKE"			6464			3933	5152	5542		386278
Control			-			-	-	-		-

	Chrysene	Benzo(b,j)fluoranthene	Benzo(k)fluoranthene	Benzo(e)pyrene	Benzo(a)pyrene	Perylene	Indeno(1,2,3-cd)pyrene	Dibenz(ac,ah)anthracene	Benzo(ghi)perylene
Smelter A1	88421	181036	287760	151220	270759		812881	683471	543978
Smelter A2	123925	141522	190861	110879	219493		413261	256020	267481
Smelter A3	201252	237531	369191	216294	293372		612604	462772	446682
Smelter B	362410	600362	738761	572083	1346157		3566701	2427022	2476866
Smelter C	1276031	432344	631691	363728	902505		1321449	946590	958255
Smelter D	161065	149670	171276	131966	276853		373933	299687	330352
Smelter E	901713	713877	862303	548341	2199152		1959675	1448692	1197896
PAH-"SPIKE"	353402	197441	159908	781133	298987		781906	472484	-
Control			-		-		-	-	-

## Appendix F.

Organic carbon:water partitioning coefficients ( $K_{OC}$ ; carbon normalized  $K_d$ ; L/kg), deduced from  $K_{OW}$ , using the Karickhoff et al. (1979) free energy relationship, and measured using POM-SPE.

### log $K_{OW}$

Naphthalene	Acenaphthylene	Acenaphthene	Fluorene	Dibenzofluorene	Phenanthrene	Anthracene	Fluoranthene	Pyrene	Benzo(a)anthracene
3.34	3.62	4	4.22		4.57	4.68	5.2	4.98	5.91

### $K_{OC}$ deduced from Karickhoff et al. 1979

Naphthalene	Acenaphthylene	Acenaphthene	Fluorene	Dibenzofluorene	Phenanthrene	Anthracene	Fluoranthene	Pyrene	Benzo(a)anthracene
1349	2570	6166	10233		22909	29512	97724	58884	501187

### $K_{OC}$ measured (MEDIANS) by POM-SPE

Naphthalene	Acenaphthylene	Acenaphthene	Fluorene	Dibenzofluorene	Phenanthrene	Anthracene	Fluoranthene	Pyrene	Benzo(a)anthracene
Smelter A1					4853296	1116238	710713	1020016	5973952
Smelter A2					1150922	1082719	1010058	1192314	6122366
Smelter A3					1543249	2468968	3752106	2994067	13543487
Smelter B					940672	559348	433780	378663	2647847
Smelter C					17116450	2129353	1083021	1371025	5755473
Smelter D					6494076	2689890	2831959	1729615	13091828
Smelter E					4307555	4463735	14228033	7967520	76758428
PAH-"SPIKE"					1026041	624335	817839	879651	-
Control					-	-	-	-	-

Cont. on next page



**log K<sub>ow</sub>**

Chrysene	Benzo( <i>b,j</i> )fluoranthene	Benzo( <i>k</i> )fluoranthene	Benzo( <i>e</i> )pyrene	Benzo( <i>a</i> )pyrene	Perylene	Indeno(1,2,3- <i>cd</i> )pyrene	Dibenz( <i>ac/ah</i> )anthracene	Benzo( <i>ghi</i> )perylene
5.81	6.12	6.11	6.13	6.58	6.5	6.22		

**K<sub>OC</sub> Deduced from Karickhoff et al. 1979**

Chrysene	Benzo( <i>b,j</i> )fluoranthene	Benzo( <i>k</i> )fluoranthene	Benzo( <i>e</i> )pyrene	Benzo( <i>a</i> )pyrene	Perylene	Indeno(1,2,3- <i>cd</i> )pyrene	Dibenz( <i>ac/ah</i> )anthracene	Benzo( <i>ghi</i> )perylene
398107	812831	794328	831764	2344229	1949845	1023293		

**K<sub>OC</sub> Measured (MEDIANS) by POM-SPE**

Chrysene	Benzo( <i>b,j</i> )fluoranthene	Benzo( <i>k</i> )fluoranthene	Benzo( <i>e</i> )pyrene	Benzo( <i>a</i> )pyrene	Perylene	Indeno(1,2,3- <i>cd</i> )pyrene	Dibenz( <i>ac/ah</i> )anthracene	Benzo( <i>ghi</i> )perylene
Smelter A1	7130752	14599667	23206454	12195155	21835413	65554898	55118643	43869210
Smelter A2	10413833	11892597	16038776	9317523	18444774	34727854	21514307	22477363
Smelter A3	12657341	14939041	23219539	13603423	18451039	38528563	29105173	28093214
Smelter B	5361091	8881095	10928419	8462768	19913562	52761844	35902691	36640037
Smelter C	23370535	7918386	11569441	6661679	16529398	24202370	17336820	17550463
Smelter D	12201914	11338651	12975459	9997433	20973719	28328282	22703527	25026630
Smelter E	66302441	52490939	63404660	40319221	161702364	144093717	106521466	88080565
PAH-"SPIKE"	-	31339829	25382271	-	47458176	124112113	74997451	-
Control	-	-	-	-	-	-	-	-

## Appendix G.

Bioconcentration factors (BCFs) deduced from  $K_{ow}$  using the equations described in the Technical Guidance Document (TGD): For  $\log K_{ow} < 6$ :  
 $\log BCF = 0.85 \times \log K_{ow} - 0.70$ ; For  $\log K_{ow} > 6$ :  $\log BCF = -0.20 \times \log K_{ow}^2 + 2.74 \times \log K_{ow} - 4.72$

### log $K_{ow}$

Naphthalene	Acenaphthylene	Acenaphthene	Fluorene	Dibenzotiofene	Phenanthrene	Anthracene	Fluoranthene	Pyrene	Benzo(a)anthracene
3.34	3.62	4	4.22	4.57	4.68	5.2	4.98	5.91	

### BCF

Naphthalene	Acenaphthylene	Acenaphthene	Fluorene	Dibenzotiofene	Phenanthrene	Anthracene	Fluoranthene	Pyrene	Benzo(a)anthracene
138	238	501	771	1529	1897	5248	3412	21062	

### log $K_{ow}$

Chrysene	Benzo(b,j)fluoranthene	Benzo(k)fluoranthene	Benzo(e)pyrene	Benzo(a)pyrene	Perylene	Indeno(1,2,3-cd)pyrene	Dibenz(ac/ah)anthracene	Benzo(ghi)perylene
5.81	6.12	6.11	6.13	6.58	6.5	6.22		

### BCF

Chrysene	Benzo(b,j)fluoranthene	Benzo(k)fluoranthene	Benzo(e)pyrene	Benzo(a)pyrene	Perylene	Indeno(1,2,3-cd)pyrene	Dibenz(ac/ah)anthracene	Benzo(ghi)perylene
17318	36134	35891	36376	44660	43652	38470		

## Appendix H.

Predicted biotaconcentrations calculated from sediment concentrations (Appendix A), POM-SPE deduced  $K_{ds}$  (Appendix E) and BCF (Appendix G):  
 $C_{biota} = (C_s/K_d) \times BCF$

	Naphthalene	Acenaphthylene	Fluorene	Dibenzofluorene	Phenanthrene	Anthracene	Fluoranthene	Pyrene	Benzo(a)anthracene
Smelter A1	2.0	3.8	226.3	67.4	65.4				
Smelter A2	21.2	10.2	266.3	113.0	147.4				
Smelter A3	12.5	2.1	30.8	22.2	19.6				
Smelter B	336.7	140.5	6264.0	4265.3	2588.7				
Smelter C	36.0	141.9	4970.0	1732.0	4088.4				
Smelter D	9.3	7.5	182.5	179.3	115.8				
Smelter E	33.9	8.1	57.0	56.7	26.2				
PAH-"SPIKE"	130.1	154.3	733.4	314.0					
Control									

	Chrysene	Benzo(b,j)fluoranthene	Benzo(k)fluoranthene	Benzo(e)pyrene	Benzo(a)pyrene	Perylene	Indeno(1,2,3-cd)pyrene	Dibenz(ac/ab)anthracene	Benzo(ghi)perylene
Smelter A1	60.7	145.7	27.4	36.3	14.3	5.2	21.2		
Smelter A2	153.7	459.6	97.8	94.5	77.8	35.8	120.8		
Smelter A3	23.2	92.8	19.4	33.5	24.8	8.4	33.6		
Smelter B	1576.9	3972.4	874.5	810.7	288.0	120.5	372.8		
Smelter C	1900.1	12536.7	2499.9	2902.0	1419.4	553.4	1565.7		
Smelter D	150.5	941.6	272.4	289.1	226.9	75.7	256.2		
Smelter E	32.6	131.6	37.9	26.5	29.6	10.8	41.7		
PAH-"SPIKE"	62.2	76.3		30.4	12.6	18.5			
Control									

## Appendix I.

Predicted biotaconcentrations calculated from sediment concentrations and organic content ( $f_{oc}$ ; Appendix A), Karickhoff et al. (1979) deduced  $K_{oc}$  (Appendix F) and BCF (Appendix G):  $K_d = K_{oc} \times f_{oc}$ ;  $C_{biota} = (C_s/K_d) \times BCF$

	Naphthalene	Acenaphthylene	Acenaphthene	Fluorene	Dibenzofluorene	Phenanthrene	Anthracene	Fluoranthene	Pyrene	Benzo(a)anthracene
Smelter A1	18.9		91.8	49.8	430.7	1065.9	145.1	1645.7	1168.2	779.5
Smelter A2	94.4		198.1	120.3	1065.9	839.7	372.7	2752.9	2288.5	1801.0
Smelter A3	102.7		194.3	104.2	839.7	13825.5	177.9	1182.1	1129.7	528.6
Smelter B	2416.4	68.6	2525.1	1783.1	13825.5	26898.6	2662.0	27804.9	27428.6	13676.5
Smelter C	5422.6	220.7	5508.2	3725.4	26898.6	681.6	10240.6	55080.2	40326.5	46950.2
Smelter D	208.8	15.4	677.4	302.5	2629.8	6381.2	1228.7	8292.4	7668.9	3024.5
Smelter E	1051.0	19.1	1912.5	997.1	6381.2	5828.0	3264.4	6137.5	4690.6	4017.0
PAH-"SPIKE"	162.1		206.4	215.2	52.5			80.6	75.9	326.9
Control	58.3									22.0

	Chrysene	Benzo(b,j)fluoranthene	Benzo(k)fluoranthene	Benzo(a)pyrene	Benzo(e)pyrene	Perylene	Indeno(1,2,3-cd)pyrene	Dibenz(ac/ab)anthracene	Benzo(ghi)perylene
Smelter A1	1087.5	2617.1	801.6	952.3	399.5	399.5	148.0	909.5	
Smelter A2	4021.1	6724.3	1974.4	2094.8	1152.7	1152.7	395.1	2653.7	
Smelter A3	738.7	1705.5	568.3	742.7	407.4	407.4	125.3	922.1	
Smelter B	21235.7	43402.7	12031.1	19408.6	6481.9	6481.9	2218.9	13347.0	
Smelter C	111541.2	122128.9	36411.6	57671.3	14654.7	14654.7	4920.3	26852.9	
Smelter D	4613.8	13134.4	4449.9	7289.0	2742.2	2742.2	881.9	6265.7	
Smelter E	5437.6	8498.7	3023.3	5145.2	1821.1	1821.1	592.6	3593.6	
PAH-"SPIKE"	303.8	2399.2	2438.5	1735.5	665.3	665.3	710.7	220.8	
Control	49.7	76.2	22.6	32.3	15.0	15.0		19.7	

## Appendix J.

Biota to sediment accumulation factors (BSAFs) measured for the polychaete *Nereis diversicolor*.

### MEDIANS:

	Naphthalene	Acenaphthylene	Acenaphthene	Fluorene	Dibenzofluorene	Phenanthrene	Anthracene	Fluoranthene	Pyrene	Benzo(a)anthracene
Smelter A1		0.0603		0.1263	0.2677	0.0290	0.0681	0.3156	0.1744	0.0338
Smelter A2				0.0514	0.0724	0.0281	0.0543	0.1447	0.1280	0.0262
Smelter A3		0.0222				0.0066		0.0181	0.0293	0.0089
Smelter B	0.0634	0.1065		0.0058	0.0123	0.0121	0.0423	0.6519	0.4489	0.2458
Smelter C		0.0988		0.0055	0.0642	0.0067	0.0960	1.2618	0.6424	0.4633
Smelter D				0.0166	0.0436	0.0111	0.0541	0.1609	0.3050	0.0702
Smelter E				0.0063	0.0060	0.0025	0.0040		0.0143	0.0012
PAH-"SPIKE"										
Control		0.2923		0.1299	0.4027	0.4724	0.1340	0.2706	0.2547	

	Chrysene	Benzo(b,j)fluoranthene	Benzo(k)fluoranthene	Benzo(e)pyrene	Benzo(a)pyrene	Perylene	Indeno(1,2,3-cd)pyrene	Dibenz(ac/ah)anthracene	Benzo(g,h,i)perylene
Smelter A1	0.0527	0.0392	0.0142	0.0533	0.0086		0.0115	0.0101	0.0150
Smelter A2	0.0207	0.0275	0.0141	0.0423	0.0124	0.0152	0.0119	0.0140	0.0175
Smelter A3	0.0072	0.0133	0.0067	0.0211			0.0072		0.0104
Smelter B	0.1101	0.2048	0.1221	0.2497	0.1099	0.1131	0.0735	0.0731	0.0986
Smelter C	0.1285	0.3640	0.1752	0.3584	0.1963	0.2202	0.1346	0.1499	0.1812
Smelter D	0.0607	0.1843	0.0774	0.2614	0.0713	0.0832	0.0523	0.0478	0.0772
Smelter E	0.0030	0.0061	0.0028	0.0086	0.0015		0.0026	0.0032	0.0042
PAH-"SPIKE"									
Control		0.0229	0.0120		0.0094		0.0071	0.0091	

## Appendix K.

Biota to sediment accumulation factors (BSAFs) measured for the gastropod *Hinia reticulata*.

### MEDIANS:

	Naphthalene	Acenaphthylene	Acenaphthene	Fluorene	Dibenzofluorene	Phenanthrene	Anthracene	Fluoranthene	Pyrene	Benzo(a)anthracene
Smelter A1	88.3575					0.2540		0.5620	0.1130	0.0389
Smelter A2	7.2636					0.0407		0.0892	0.0344	0.0077
Smelter A3	9.5234			0.1205		0.0467		0.0299	0.0239	
Smelter B	0.1284	0.0549		0.0501	0.0558	0.0554	0.0828	1.3634	0.6627	0.1446
Smelter C	0.0377	0.0341		0.0058	0.0585	0.0067	0.0706	1.0969	0.4894	0.3161
Smelter D	0.8148					0.0187	0.0258	0.1148	0.0838	0.0152
Smelter E	0.8571					0.0226		0.0119	0.0136	0.0078
PAH-"SPIKE"						0.1184	0.0381	0.1108	0.0684	
Control	17.9730					1.3071		0.2342	0.2270	

	Chrysene	Benzo(b,j)fluoranthene	Benzo(k)fluoranthene	Benzo(e)pyrene	Benzo(a)pyrene	Perylene	Indeno(1,2,3-cd)pyrene	Dibenz(ac,ah)anthracene	Benzo(g,h,i)perylene
Smelter A1	0.0678	0.0231	0.0658	0.0899					
Smelter A2	0.0039	0.0071	0.0139	0.0234	0.0069		0.0076	0.0085	0.0101
Smelter A3	0.0108	0.0083	0.0139	0.0192			0.0094		0.0136
Smelter B	0.0562	0.1105	0.1841	0.2802	0.0795	0.0831	0.0749	0.0851	0.1049
Smelter C	0.0646	0.1649	0.1435	0.1940	0.0901	0.0963	0.0451	0.0526	0.0595
Smelter D	0.0213	0.0214	0.0544	0.0851	0.0207	0.0263	0.0165	0.0178	0.0229
Smelter E	0.0096	0.0113	0.0155	0.0249	0.0083	0.0117	0.0117	0.0109	0.0178
PAH-"SPIKE"		0.0107	0.0161	0.0397	0.0113		0.0122		0.0363
Control									

## Appendix L.

Biota to sediment accumulation factors (BSAFs) measured for the bivalve *Nuculoma tenuis*.

### MEDIANS:

	Naphthalene	Acenaphthylene	Acenaphthene	Fluorene	Dibenzofluorene	Phenanthrene	Anthracene	Fluoranthene	Pyrene	Benzo(a)anthracene
Smelter A1		0.4996			1.4194	0.3338	1.5897	5.6896	4.9600	5.3913
Smelter A2		0.0888			0.2147	0.1743	0.4801	1.0659	1.2529	1.4674
Smelter A3		0.1902		0.3066	0.2038	0.2048	0.3340	0.5094	1.1657	1.4455
Smelter B	0.4027	0.0925		0.0944	0.1212	0.1130	0.3082	2.6711	3.3710	2.3209
Smelter C	0.2861	0.3422		0.0938	0.5370	0.1007	1.2734	7.3478	4.5812	3.1133
Smelter D	5.6471	0.1871		0.2271		0.1867	0.9151	1.7620	3.8824	2.1251
Smelter E		0.0502		0.0549	0.0481	0.0476	0.0927	0.0883	0.3949	0.1807
PAH-"SPIKE"						1.0107	0.5211	1.0809	1.2353	
Control									1.1709	

	Chrysene	Benzo(b)fluoranthene	Benzo(k)fluoranthene	Benzo(e)pyrene	Benzo(a)pyrene	Perylene	Indeno(1,2,3-cd)pyrene	Dibenz(ac)anthracene	Benzo(g,h)perylene
Smelter A1	4.2051	4.7910	4.3357	3.9398	2.7085	2.0573	2.4458	2.3265	2.4376
Smelter A2	0.7472	1.7721	1.6751	1.5335	1.2483	1.0632	1.5165	1.5189	1.4459
Smelter A3	1.5168	2.7250	2.5295	2.4693	1.2492	0.6731	1.9840	2.0572	2.1620
Smelter B	0.4576	1.7434	1.5981	1.5200	1.1027	0.8898	0.8755	0.9338	0.8690
Smelter C	0.8478	1.8991	1.2769	1.6659	1.0990	0.9609	0.6783	0.7913	0.7101
Smelter D	1.3588	5.0769	4.4796	4.3676	3.1765	2.5412	3.0650	2.7624	2.6471
Smelter E	0.2182	1.0105	0.8831	1.0303	0.3284	0.2627	0.6182	0.6525	0.7846
PAH-"SPIKE"		0.5886	0.6213		0.4299		0.3201	0.4076	
Control		1.4389	1.4000	2.0160			2.2485		8.2727

## Appendix M.

Biota to sediment accumulation factors (BSAFs) predicted from the Karickhoff et al. (1979) free energy relationship (BSAF =  $\frac{K_{ow} \cdot C_w}{0.62 \cdot K_{ow} \cdot C_w} = 1.62$ ), and BSAFs predicted from sediment concentrations and organic content ( $f_{oc}$ ; Appendix A), POM-SPE deduced  $K_{ds}$  (Appendix E) and  $K_{ow}$  ( $K_{lipid} = K_{ow}$ ):

$$BSAF = \frac{C_{lipid}}{C_{oc}} = \frac{K_{lipid} \cdot C_w}{C_s} \left( \frac{C_s}{f_{oc}} \right) \text{ where } C_w = C_s / K_d$$

### BSAF predicted from Karickhoff et al. 1979

	1.62	1.62	1.62	1.62	1.62	1.62	1.62	1.62	1.62
Naphthalene	Acenaphthylene	Acenaphthene	Fluorene	Dibenzofluorene	Phenanthrene	Anthracene	Fluoranthene	Pyrene	Benzo(a)anthracene

### BSAF predicted by POM-SPE

	0.0077	0.0429	0.2230	0.0936	0.1361
Smelter A1	0.0323	0.0442	0.1569	0.0801	0.1328
Smelter A2	0.0241	0.0194	0.0422	0.0319	0.0600
Smelter A3	0.0395	0.0856	0.3654	0.2522	0.3070
Smelter B	0.0022	0.0225	0.1463	0.0697	0.1412
Smelter C	0.0057	0.0178	0.0560	0.0552	0.0621
Smelter D	0.0086	0.0107	0.0111	0.0120	0.0106
Smelter E	0.0362	0.0767	0.1938	0.1086	
PAH-"SPIKE"					
Control					

Cont. on next page



**BSAF predicted from Karickhoff et al. 1979**

	1.62	1.62	1.62	1.62	1.62	1.62	1.62	1.62	1.62
Chrysene	Benzo( <i>b,j</i> )fluoranthene	Benzo( <i>k</i> )fluoranthene	Benzo( <i>e</i> )pyrene	Benzo( <i>a</i> )pyrene	Perylene	Indeno(1,2,3- <i>cd</i> )pyrene	Dibenz( <i>ac/ah</i> )anthracene	Benzo( <i>ghi</i> )perylene	1.62

**BSAF predicted by POM-SPE**

	Chrysene	Benzo( <i>b,j</i> )fluoranthene	Benzo( <i>k</i> )fluoranthene	Benzo( <i>e</i> )pyrene	Benzo( <i>a</i> )pyrene	Perylene	Indeno(1,2,3- <i>cd</i> )pyrene	Dibenz( <i>ac/ah</i> )anthracene	Benzo( <i>ghi</i> )perylene
Smelter A1	0.0905	0.0903	0.0555	0.0618	0.0731	0.1095	0.0580	0.0574	0.0378
Smelter A2	0.0620	0.1108	0.0803	0.0731	0.0731	0.1095	0.1095	0.1470	0.0738
Smelter A3	0.0510	0.0882	0.0555	0.0731	0.0731	0.0987	0.0987	0.1087	0.0591
Smelter B	0.1204	0.1484	0.1179	0.0677	0.0677	0.0721	0.0721	0.0881	0.0453
Smelter C	0.0276	0.1665	0.1113	0.0816	0.0816	0.1571	0.1571	0.1824	0.0946
Smelter D	0.0529	0.1163	0.0993	0.0643	0.0643	0.1342	0.1342	0.1393	0.0663
Smelter E	0.0097	0.0251	0.0203	0.0083	0.0083	0.0264	0.0264	0.0297	0.0188
PAH-"SPIKE"		0.0421	0.0508	0.0284	0.0284	0.0306	0.0306	0.0422	
Control									